# Formation and differents magma interaction in systems of fluid-melt-crystal

## Asavin A.M. Multi-magmas numerical model crystallization differentiation primary melts of the oceanic island volcanic series

V. I. Vernadsky Institute of Geochemistry and Analytical Chemistry RAS, Moscow

**Abstract**. Were calculated models, to simulate the processes of fractional crystallization in alkaline basalt volcanic series of oceanic islands of the Atlantic ocean. Calculations demonstrate independence of the ankaramite and alkali olivine basalt melts. Trachybasalts and trachyandesites can be obtained only from the ankaramite melts. Formation of the phonolite due either to the processes of secondary melting and assimilation of a siliceous volcanic products, or by fractionation of basanite melts with high alkali content, or similar tephrite.The simulation shows that the process of formation of intraplate volcanic centers in the oceanic plate was multi act and primary mantle-derived magmas have formed a number of independent primary melts.

*Key word: oceanic island, volcanic series, alkaline magmatism, fractional crystallization, primary melts.*

**Citation:** Asavin, A.M. (2013). Multi-magmas numerical model crystallization differentiation primary melts of the oceanic island volcanic series.

**Introduction.** One of the main theory to explain the formation of the volcanic series is the process of fractional crystallization of the primary mantle melts. However, the number of numerical models of the formation of the natural volcanic series to date is limited [Thy et al., 1991; Hoernle & Schmincke 1993; Fretzdorff et al., 1996; Ablay et al., 1998; Kar et al., 1998; Torres et al., 2010; Kawabata et al., 2011; Hildner et al., 2011; Legendre et al., 2005].

The previous data on the composition of rocks and minerals in the rocks of volcanic series Tristan da Cunha Islands, Gran Canaria, Saint Helena [Barsukov et al., 1979; Kogarko et al., 1985; Asavin et al., 1994; Asavin et al., 1997], and a number of new analyzes allow for detailed modeling processof fractional crystallizationof the formation of volcanic rocks forming the data series.

Software simulated equilibrium between the source and destination melt achieved by the addition or subtraction of minerals crystallize at this stage of fractionation. The compositions of these minerals were estimated on the composition of phenocrysts in the motherand daughter rocks. In addition, we used data on the composition of the groundmass. The calculation was performed on eight main chemical components - $SiO_2$, $TiO_2$, $Al_2O_3$, FeO (total iron calculated as FeO), MgO, CaO, $Na_2O$, $K_2O$. We solve systems of linear equations by the method of least squares to calculate coefficients ofminerals included in the equation, and calculated the mean square residual error of the solution ($\Sigma R^2$).

Variants of solutions to equations that have characterized the positive decision were square residual error value less than 1. Otherwise, errors in determining the phase fraction in equation is much greater than.50% (up to 100% and more) and thus the system had not reasonable (accurate comparable determination of chemical components) solutions.

**Result.** Calculation of more than 500 combinations of paired volcanic rocks (parent - daughter) and phenocrysts are allowed to allocate satisfying and not satisfying the process of crystallization differentiation options for the formation of natural melts.

It should be noted that earlier in [Barsukov et al., 1979], similar calculations were performed using the average of the rocks. In many cases, used no equilibrium minerals with the composition groundmass of the rock. Despite the general conclusion of this article that "a series of alkaline volcanic rocks of the South Atlantic islands were formed by processes of fractional crystallization differentiation" in the numerical models series of each island there is a bad calculation ($\Sigma R^2 > 1$) for one of the steps of fractionation. The authors speculated that this is due to the use of non-equilibrium phenocrysts, so when setting this work we hoped that when re-calculated using the compositions of equilibrium with minerals will improve the quality of calculations. Also in the contrary of the old model calculations, we used a real natural rock compositions (not an average composition) of initial and final differentiates. Due to the limited volume of this publication format, we do not present the analysis of rocks and minerals used in the calculations, and the actual results of the calculations are presented Fig. 1, and the successful variants are shown in Table 1. It should be noted that some calculation were $\Sigma R^2 < 1$, but were negative mineral proportion, so these calculations we also relates to a failure.

**Table 1**. Equations coefficients satisfying the mass balance of the main components among members volcanic series on St. Helena island (CE), Tristan da Cunha island (TK), Gran Canaria island (12879); F - fraction of residual melt, ΣR2 sum of the mean square residual error in the calculation.

| Step of the differentiation | № Sample | | Cumulus minerals proportion from equation (rel. %) | | | | | | |
|---|---|---|---|---|---|---|---|---|---|
| primary melt -differentiate | parent | daughter | F | Ol | Cpx | Mgt | Pl | Fsp | ΣR² |
| Ankaramite – ankaramitbasalt | TK34 | TK40 | 58.89 | 4.15 | 26.38 | 6.66 | 4.34 | | 0.28 |
| | TK46 | TK41 | 60.09 | 16.55 | 18.4 | 1.01 | 3.46 | | 0.78 |
| Ankaramite – alkaline Ol basalt | TK34 | TK7 | 50.27 | 3.27 | 44.9 | 1.42 | 1.58 | | 0.3 |
| | TK41 | TK38 | 64.79 | 3.03 | 21.84 | 6.42 | 3.81 | | 0.22 |
| | TK46 | TK38 | 44.74 | 14 | 32.76 | 6.97 | 1.95 | | 0.35 |
| Ankaramite - trachybasalt | CE3 | CE14 | 44.35 | 13.83 | 37.12 | | 4.12 | | 0.67 |
| | TK40 | TK33 | 75.29 | 10 | 2.41 | 3.31 | 9.91 | | 0.94 |
| | TK40 | TK42 | 80 | 9.46 | | 2.88 | 8.09 | | 0.13 |
| | TK40 | TK9 | 65.5 | 11 | 6.43 | 5.27 | 11.61 | | 0.9 |

| Step of the differentiation | № Sample | | Cumulus minerals proportion from equation (rel. %) | | | | | | |
|---|---|---|---|---|---|---|---|---|---|
| alkaline Ol basalt - trachybasalt | TK38 | TK2 | 98.36 | 1.04 | 0.45 | 0.04 | | | 0.43 |
| Trachybasalt - trachyandesite | TK22 | TK50 | 59.8 | 3.15 | 17.06 | 8.17 | 11.09 | | 0.47 |
| | TK33 | TK50 | 65.08 | 2.67 | 14.29 | 6.15 | 11.42 | | 0.78 |
| | TK4 | TK49 | 74.29 | | 13.64 | 6.3 | 4.32 | | 0.64 |
| | 12879 | 12879om | 58.83 | | 24.34 | 3.29 | 8.28 | | 0.83 |
| | TK42 | TK49 | 75.4 | 0.63 | 15.58 | 4.22 | 4.08 | | 0.67 |
| Trachybasalt - Trachyte | TK22 | TK15 | 46.74 | 3.11 | 22.61 | 10.95 | 16.53 | | 0.89 |
| | TK22 | TK19 | 54.01 | 3.31 | 19.04 | 9.1 | 13.55 | | 0.29 |
| | TK4 | TK19 | 49.36 | 0.34 | 19.03 | 9.9 | 15.28 | 3.3 | 0.97 |
| Trachyandesite - Trachyte | TK50 | TK19 | 90.38 | | 3.62 | 1.58 | 3.95 | | 0.08 |

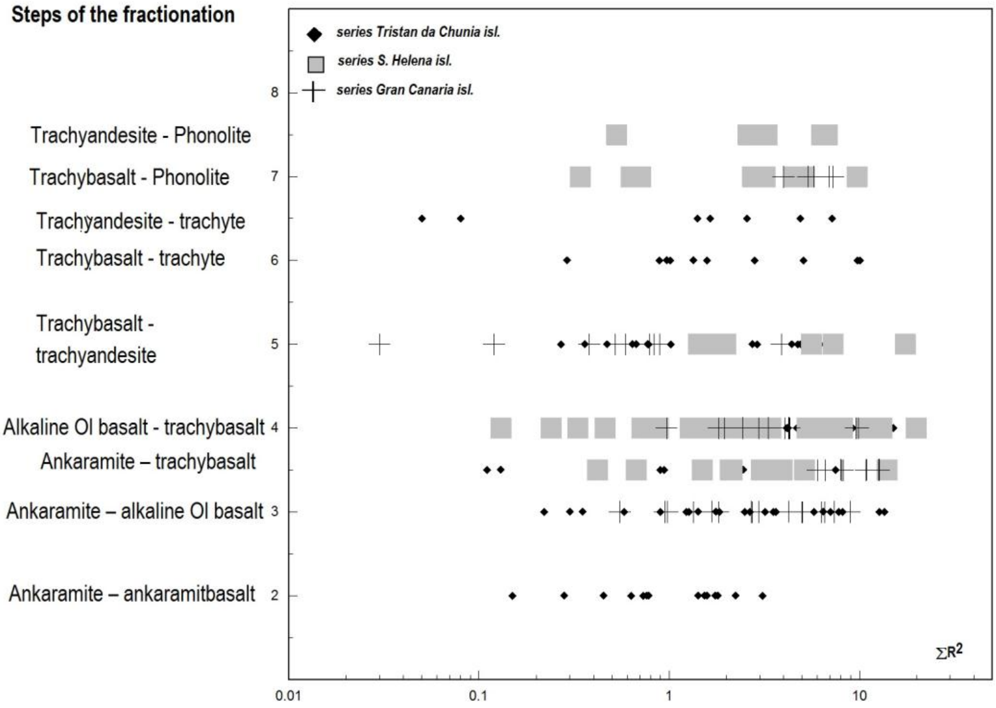

**Fig. 1.** The calculations ΣR2 in different models of the steps of fractionation

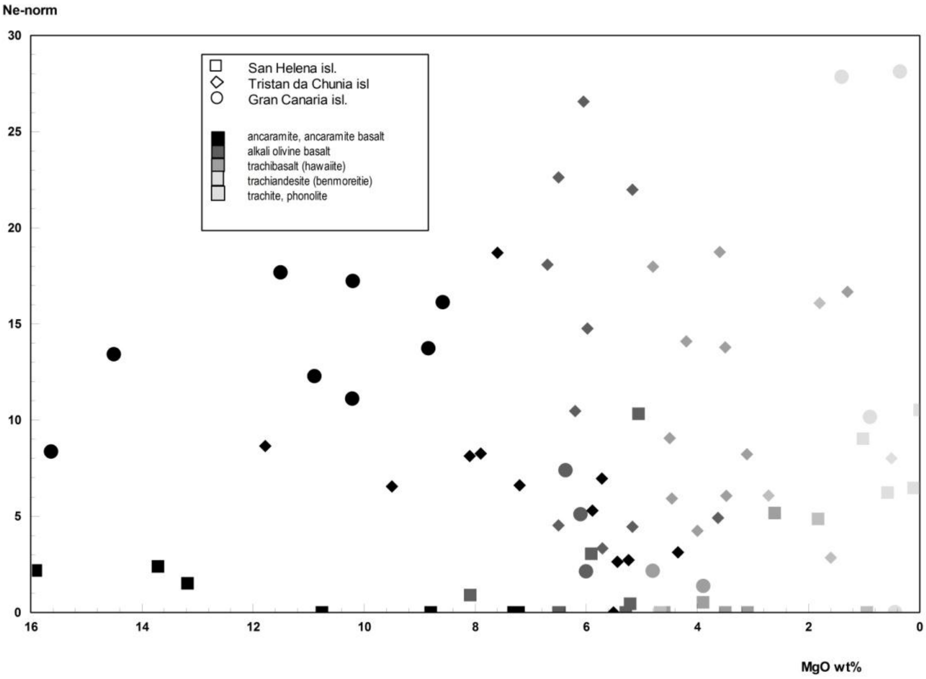

**Fig. 2.** Variations of the contents of normative nepheline (CIPW) in the volcanic rocks

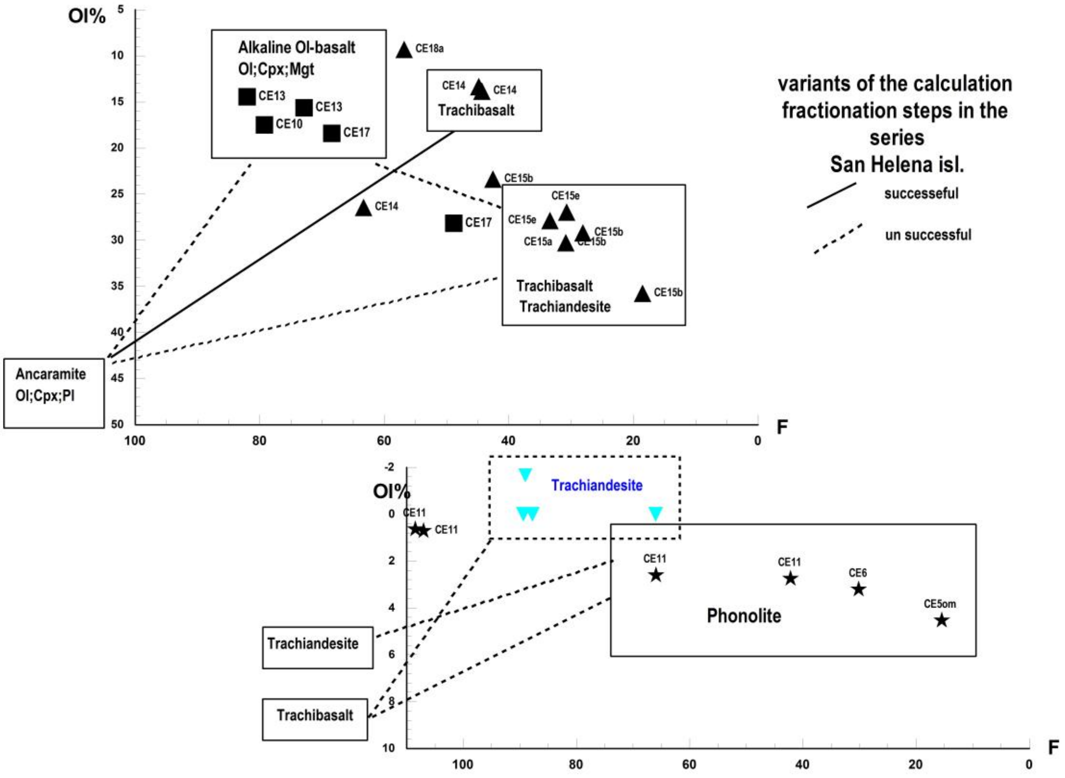

**Fig. 3.** Scheme of calculations for fractionation stages of volcanic series on St. Helena isl. F - fraction of residual melt in the model equation, Ol% - the proportion of olivine in the calculation (the axis for both parameters are inverted for clarity)

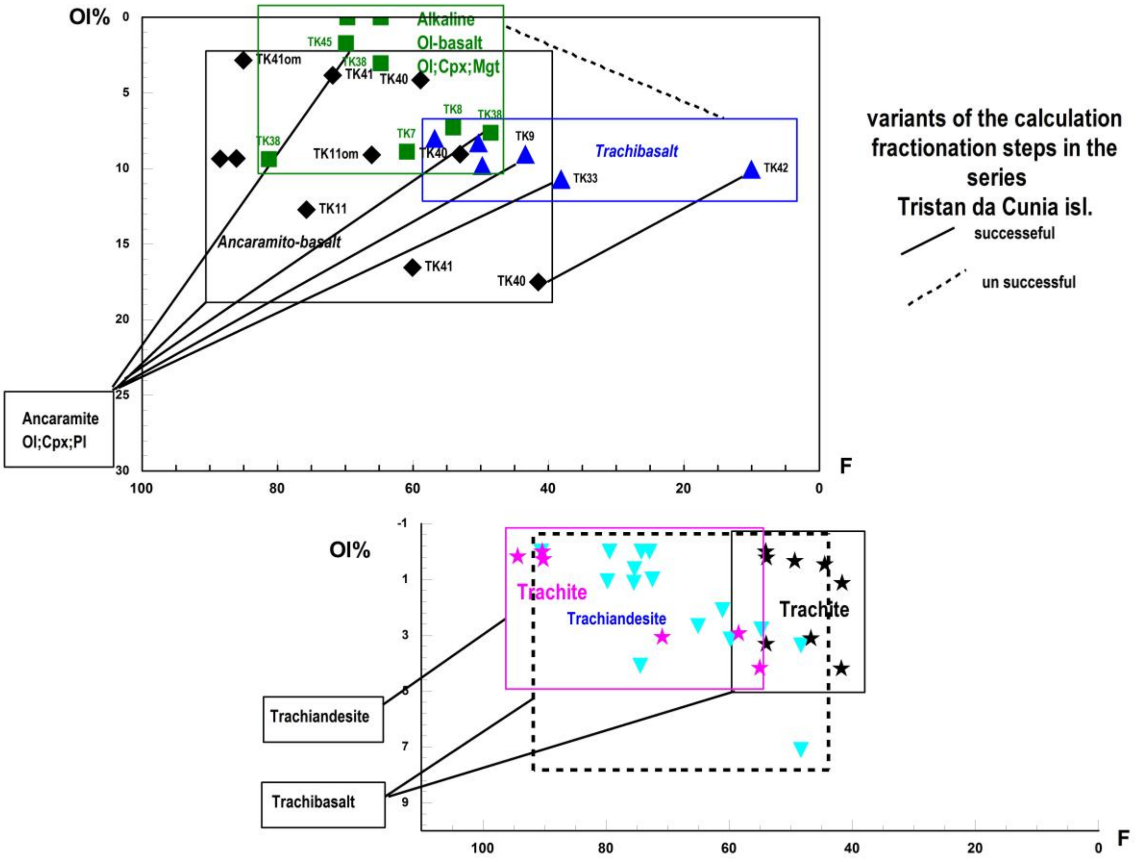

**Fig. 4.** Scheme of calculations for fractionation stages of volcanic series on Tristan da Cunha isl. (axes parameters the same as in the Fig.3)

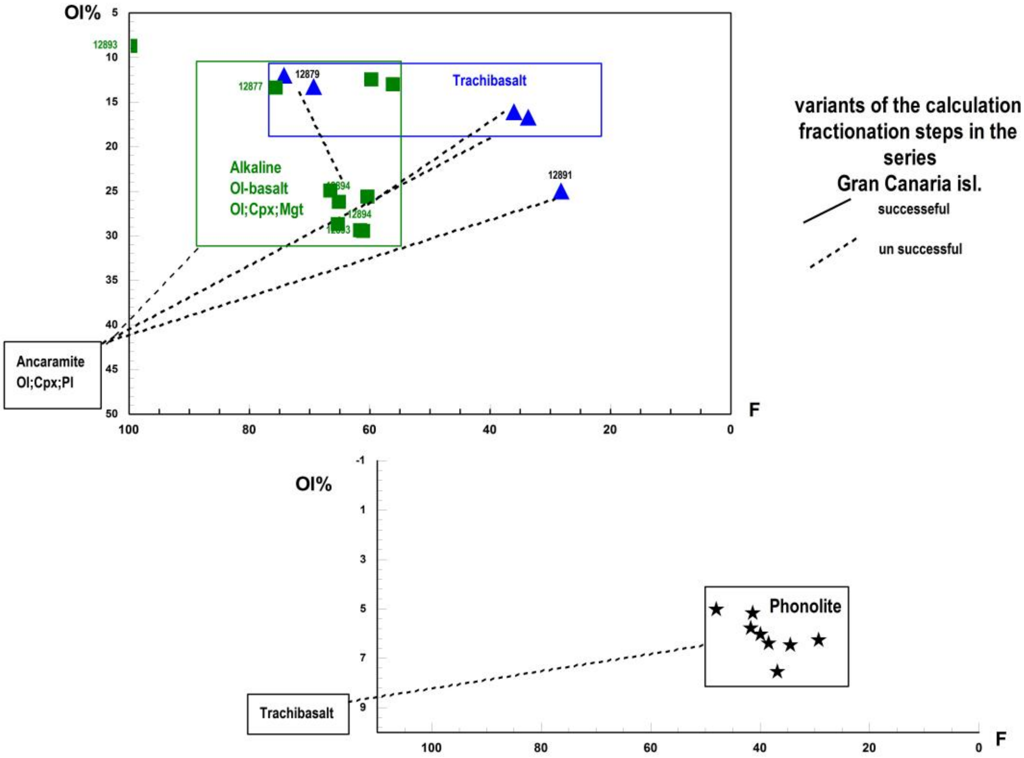

**Fig. 5.** Scheme of calculations for fractionation stages of volcanic series on Gran Canaria isl. (axes parameters the same as in the Fig.3)

Series Sn. Helena isl. represented next steps: ankaramite – alkaline olivine basalt-trachybasalt - trachyandesite - phonolite. All calculations were given large discrepancy, the proportion of magnetite is small and usually negative. The exception is the transition CE3-SE14 ankaramite - trachybasalt.

Series Tristan da Cunha isl. presented steps: ankaramite – alkaline olivine basalt - trachybasalt - trachyte. It was possible to calculate the transitions ankaramite - trachybasalt; trachybasalt - trachyandesite; trachybasalt - trachyte, trachyandesite - trachyte; Differentiation step ankaramite - alkaline basalt for most pairs have been unsuccessful.

The large discrepancy in the calculations argue that by fractionation process impossible to obtain such melts as from one another. The main conclusion from these calculations is the autonomy and independence of ankaramitic and alkaline olivine basalt melts. It should be noted that we know of the work on modeling of crystallization differentiation in the formation of high-Mg volcanic series records (> 7-8% MgO) rocks formed only in a limited number of publications [Zielinski & Frey 1970; Clague et al., 1980; Flower 1973; Le Roex et al., 1990; Kawabata & Hanyu 2005].

These works are not successful calculations proving relation between ankaramite-picritic melts with alkaline basalts. In this regard, the authors as well as we consider ankaramite melts as independent products of partial melting of the mantle, which differ from basanitic and alkaline basaltic magmas on the different portion and conditions of the melting of the mantle. In Fig. 2 shows that the range of the content in our normative nepheline (by CIPW norm) similar melts can vary quite substantially, which cannot be explained by fractional crystallization processes. Available in our analyzes show that in a series of islands Gran Canaria and St Helens in alkaline olivine basalts percentage normative nepheline falls while reducing the magnesium content.

This fact and closeness the compositions (by the macro components) and explains to failure in the calculations model when trying to deduce the alkaline basalts from ankaramitic melts. More evolving volcanic rocks: trachybasalt and trachyandesite (hawaiites) cannot always be linked with ankaramitic melts. Only in a series on St. Helena Island and Tristan da Cunha managed to spend a good account in this step fractionation. Of alkaline olivine basalt failed to produce intermediate differentiates - trachybasalt and trachyandesite. At this stage of fractionation are formed very close compositions of rocks, which is reflected in the calculation of large values of F.

Published data indicate that the high-Mg melts basanitic able to form a highly differentiated alkaline melts hawaiites, mugearite and phonolite [Ellis 1976; Price & Chappell 1975; Fitton & Hughes 1977; Garcia et al., 1986; Le Roex et al., 1990; Wilkinson & Hensel 1991; Kyle et al., 1992; Maaloe et al., 1992; Panter et al., 1997; Legendre et al., 2005]. Most models consider fractionation basanitic melt as high-pressure process with the participation of the fluid phase and the appearance of amphibole on the liquidus. However, for the formation of phonolite melt even these models do not always solve the problem. In a number of models for the formation of phonolite involved processes of mixing and assimilation [Wedepohl et al., 1994; Ulrich et al., 2000; Irving & Green 2008; Lucassen et al., 2013]. The study differentiates end process of evolution - phonolite, ordanshite revealed that, despite the nature of the eutectic melts, there are several possibilities of their education, which is reflected in the difference of trace elements concentration and isotopic composition of specific regions.

The formation of trachyandesite due, apparently to the evolution of ankaramitic melts not alkaline basalts. The alkali olivine basalt melt is deadlock branch line, close to the pseudo-eutectic Ol-Cpx-Pl-Mgt point.

Most researchers could not link the phonolite melts with basalt by calculation. The effect of an increase in the content of normative nepheline melt due to the effect of plagioclase and pyroxene is too small, for example in the work of [Ellis 1976] showed that an increase of 1% of the content of normative nepheline requires 20% removal of clinopyroxene. Although we were unable to connect with trachyte melt fractionation alkaline basaltic melt opportunity to the formation of more acidic, trachyte melts remains real. This most likely be formed slightly alkaline intermediate species with a lower magnesium content. As such, in the studies mentioned, numerically simulating the fractionation of alkali basaltic melt does not provide evidence of the formation of his trachyte melts.

## Conclusion

The numerical simulation of fractional crystallization of alkaline basalt volcanic series of oceanic islands showed that the volcanic rocks cannot be connected with one single process and one single petrochemical type of primary melt. There are at least three independent types of primary magmas - ankaramite- picrite, alkaline olivine basalt and basanitic.

Intermediate members of the series - trachybasalt and trachyandesite can be formed by differentiating ankaramite-picritic primary melts.

End evolution members, highly alkaline melts - phonolite, trachyphonolite, oradanshite not connected to subalkalic high-Mg magmas, and could only form from basanitic melts with high level of nepheline abundance. These conclusions lead us to a model of a melt of variable multi-source magmatic. This model rejects the idea of a single parent magmatic source of oceanic islands. We assume that the formation of the volcanic edifice of oceanic islands simultaneously there were different independent sources of melts, probably located at different depths and generating primary magma of different alkalinity.

References:

1. Ablay, G.J., M.R. Carroll, M.R. Palmer, J. Mart, R.S.J. Sparks. (1998). Basanite-phonolite lineages of the Teide-Pico Viejo volcanic complex, Teneriffe, Canary Islands. *Journal of Petrology,* V.39, N.5, pp. 905-936.
2. Asavin A.M., L. N. Kogarko, V.A. Karpushina, G.M. Kolesov, O.I. Kruchkova, D.A.Tjurin (1994). Distribution of rare lithophyle elements (Zr.Hf,Nb,Ta,Th, U ) and their ratio variations in the alkaline-basaltic ocean island series of the souther Atlantics (Gran Canaria, St.Helena, Tristan de Kunja). *Geochemistry Int.,* N. 8-9, pp. 1161-1173
3. Asavin A. M., L. N. Kogarko, O. I. Kryuchkova, D. A. Tyurin, G. M. Kolesov. (1997). The Grand Canary, Saint Helena, and Tristan da Cunha oceanic islands: variations of trace element partition coefficients in pyroxene-melt equilibria during alkaline magma evolution. *Geochem. Int.,* V. 35, pp. 415-423
4. Barsikov V. L., L. N. Kogarko, A. I. Polyakov, K. I. Ignatenko, A. I. Zinove^ev. (1979). Differentiation of basaltoid melts and formation of the volcanic rock series of the South Atlantic islands. *Geochem. Int.,* V.6, N6, pp. 1-12
5. Clague, D.A., E.D. Jackson, T.L. Wright. (1980). Petrology of Hualalai Volcano, Hawaii: Implication for Mantle Composition. *Bull. Volcanol.,* V.43, N4, pp. 641-656.
6. Ellis, D.J. (1976). High Pressure Cognate Inclusions in the Newer Volcanics of Victoria. *Contrib. Mineral. Petrol.,* V.58, pp. 149-180.
7. Fitton, J.G., and D.J. Hughes. (1977). Petrochemistry of the Volcanic Rocks of the Island of Principe, Gulf of Guinea. *Contrib. Mineral. Petrol.,* V.64, pp. 257-272.
8. Flower, M. F. J. (1973). Evolution of Basaltic and Differentiated Lavas from Anjouan, Comores Archipelago. *Contrib. Mineral. Petrol.,* V.38, pp. 237-260.
9. Fretzdorff, S., K.M. Haase, C.-D. Garbe-Schonberg. (1996). Petrogenesis of lavas from the Umu Volcanic Field in the young Hotspot Region west of Easter Island, southeastern Pacific. *Lithos,* V.38, pp. 23-40.
10. Garcia, M. O., F. A. Frey, and D. G. Grooms. (1986). Petrology of volcanic rocks from Kaula Island, Hawaii Implications for the origin of Hawaiian phonolites. *Contrib. Mineral. Petrol.,* V.94, pp. 461-471.
11. Hildner, E., A. Klugel,F.Hauff. (2011). Magma storage and ascent during the 1995 eruption of Fogo, Cape Verde Archipelago. *Contrib. Mineral. Petrol.,* V.162, pp. 751–772.
12. Hoernle, K., H. U. Schmincke. (1993). The petrology of the tholeiites through melilite nephelinites on Gran Canaria, Canary Islands: crystal fractionation, accumulation, and depths of melting. *Journal of Petrology,* V.34, N.3, pp. 573-597.
13. Irving, A. J., and D. H. Green. (2008). Phase Relationships of Hydrous Alkalic Magmas at High Pressures: Production of Nepheline Hawaiitic to Mugearitic Liquids by Amphibole-Dominated Fractional Crystallization Within the Lithospheric Mantle. *Journal of Petrology,* V.49, N.4, pp. 41-756.
14. Kar, A., B. Weaver, J. Davidson, M. Colucci. (1998). Origin of differentiated volcanic and plutonic rocks from Ascension Island, South Atlantic Ocean. *Journal of Petrology,* V.39, N.5, pp. 1009-1024.
15. Kawabata, H., T. Hanyu. (2005). Magmatic processes for producing the variations from ankaramites to phenocryst-poor basalts: an example from St. Helena Island. *Frontier Research on Earth Evolution,* V.2, pp. 1-8.
16. Kawabata, H., T. Hanyu, Jun-Ichi Qing Chang, Kimura, A. R. L. Nichols, and Y. Tatsumi. (2011). The Petrology and Geochemistry of St. Helena Alkali Basalts: Evaluation of the Oceanic Crust-recycling Model for HIMU OIB. *Journal of Petrology,* V.52, N.4, pp. 791-838.
17. Kogarko L. N., V. L. Barsikov, A. M. Asavin, A. I. Polyakov, S. M. Chernogovorova, N. A. Korovkina, G. I. Ramendik. (1986). Geochemistry of the iron-group elements during the fractional differentiation of oceanic-island alkali series. *Geochem. Int.,* V.3, N2, pp. 51-65
18. Kyle, P.R.,J. A. Moore, M. F. Thirlwall. (1992). Petrologic Evolution of Anorthoclase Phonolite Lavas at Mount Erebus, Ross Island, Antarctica. *Journal of Petrology,* V.33, N.4, pp. 849-875 .
19. Le Roex, A. P., R. A. Cliff, B. J. I. Adair. (1990). Tristan da Cunha, South Atlantic: geochemistry and petrogenesis of a basanite-phonolite lava series. *Journal of Petrology,* V.31, p 779-812.
20. Legendre, C., Maury, R.C., Savanier, D., Cotton, J., Chauvel, C., Hemond, C., Bollinger, C., Guille, G., Blais, S., Rossi, P. (2005). The origin of intermediate and evolved lavas in the Marquesas archipelago: an example from Nuku Hiva island (French Polynesia). *Journal of Volcanology and Geothermal Research,* V.143, N.4, pp. 293-317.
21. Lucassen, F., P. Dieter, F. Gerhard, R. L. Romer, P. Dulski. (2013). Cenozoic intraplate magmatism in the Darfur volcanic province: mantle source, phonolite-trachyte genesis and relation to other volcanic provinces in NE Africa. *Int. J Earth Sci Geol Rundsch.,* V.102, pp. 183–205.
22. Maaloe, S. D., J.E Smedley, P. E. Petersen, Sven, D. Garmann, and F.B. Lei. (1992). The Koloa Volcanic Suite of Kauai, Hawaii. *Journal of Petrology,* V.33, Par.4, pp. 761-784.

23. Panter, K. S., P. R. Kyle, and J. L. Smellie. (1997). Petrogenesis of a Phonolite–Trachyte Succession at Mount Sidley, Marie Byrd Land. Antarctica. *Journal of Petrology*, V.38, N.9, pp. 1225–1253.
24. Price, R.C., B.W. Chappell. (1975). Fractional Crystallisation and the Petrology of Dunedin Volcano. *Contrib. Mineral. Petrol.,* V.53, pp. 157-182.
25. Thy, P., G.E. Lofgren, P. Imsland. (1991). Melting relations and the evolution of the Jan Mayen magma system. *Journal of Petrology*, V..32, N.2, pp. 303-332.
26. Torres, P., L. C. Silva, J. Munha, R. Caldeira, J. Mata, & C. Tassinari. (2010). Petrology and Geochemistry of lavas from Sal Island: Implications for the variability of the Cape Verde magmatism. *Comunicacoes Geologicas.,* V.97, pp. 35-62.
27. Ulrich, J., V. Cajz, E. Pivec, Novak, K. Jiri, C. Nekovarik, K. Balogh. (2000). Cenozoic intraplate alkaline volcanism of western Bohemia. *Studia geoph. et geod,* V.44, 346-351.
28. Wedepohl, K. H., E. Gohn, and G. Hartmann. (1994). Cenozoic alkali basaltic magmas of western Germany and their products of differentiation. *Contrib. Mineral. Petrol.,* V.115, pp. 253.
29. Wilkinson, J.F.G. and H.D. Hensel. (1991). An analcime mugearite-megacryst association from north-eastern New South Wales: implications for high-pressure amphibole-dominated fractionation of alkaline magmas. *Contrib. Mineral. Petrol.,* V.109, pp. 240-251.
30. Zielinski, R.A. Frey. (1970). Gough Island: Evaluation of a fractional crystallization model. *Contrib. Mineral. Petrol.,* V.29, N.3, pp. 242-254.

## Klisch I., Gevorkyan R.G. The dynamic model of the formation of igneous rocks of the Harz mountains

Yerevan State University (YSU), Armenia

**Abstract.** The main content of the presented petrological-geochemical model describes the processes of migration from the original tolaidic igneous centre in the Harz Mountains from south-east to north-west. A successively change in the composition of the melt up to formation of granitoids by the ongoing progressive polygenesis, igneous displacement as well as metasomatism. As a leading force in these processes, the amplification of tectonic stresses along the Variscian sliding zone is considered.

*Key words: model, Harz, granitoide, palingenese, metasomatose, tectonic stresses, Variscian sliding zone.*

**Citation:** Klisch I., R.G. Gevorkyan (2013). The dynamic model of the formation of igneous rocks of the Harz mountains. *Vestni*

The Harz mountain range is located in the northern part of Germany and has a position within the Rhenohercynian zone between the Rhenish Massif and the Flechtingen Hills [Gevorkian R.G., Klisch I., 2009].

The rosscks of the Harz Mountains form a solid, strong metamorphic upper-Paleozoic complex like a horst, in which mainly the Devonian and older-Carboniferous formations are represented. The geological structure of the Harz Mountains is divided into three big morphological units, which are marked by the three regional fault zones.

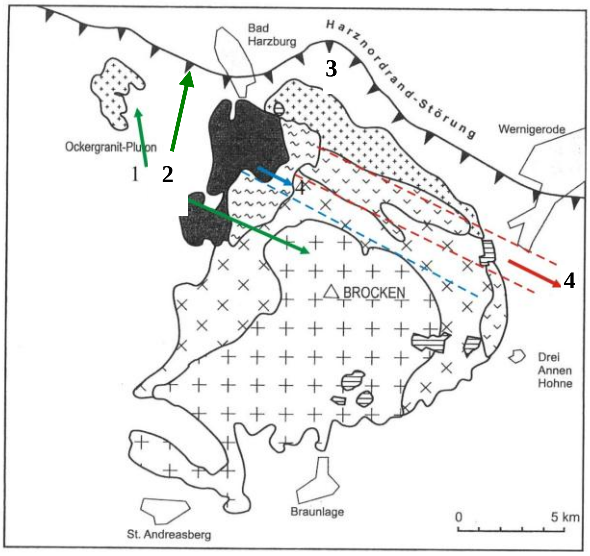

**Fig. 1:**

1. Separation of Oker Massif.
2. Displacement in the Rhine direction (SW-NE) due to increase in stress.
3. Separation of massif Ilzeshteyna.
4. Direction of maxmial tectonic stress due to due to the introduction tholeiite-basaltic melt. Displacement in the Hercynian (NW–SE) direction.

Igneous rocks in the Harz Mountains are known as: Ramberg Massif, Brocken Massif with Harzburg gabbro, Oker Massif.

Within the Harz Mountains there exist 14 geological units. Their recent bounds were formed during the entire evolution in the early stages of the orogeny, sedimentation and magmatic events [Bachmann G.H., Ehling B.C., Eichner R., Schwab M., 2008].

**Magmatism.** The complicated mechanism of magmatic events in the Harz Mountains can not only be analyzed with the help of thorough studying of effusive and intrusive fazies, but also with using of detailed tectono-plutonical formation analyses.

1. *Gabbro-Harzburgit formation. Series.* The rocks of this group in the Harz Mountains are typical associations of gabbro and harzburgit with the upper-Paleozoic with the pyroclastic equivalents of volcaniclastic-sedimentation complex spilite-diabase composition for the initial phase of evgeosyncline (sedimentation in the basin). These are metabasalts of Silurian up to diabases, spilite and their pyroclastics of middle-Devonian and to the near-surface intrusive massive diabase and gabbro-diabase of the lower Carboniferous.

2. *Banatit-Gabbro formation. Banatit-Series.* The granitoids of the Harz Mountains have a 10 times larger spread area than the ultrabasite-basite. The complex-differentiated massif of Brocken, Ramberg and Oker play a significant role, which are expanded with the whole complex of intrusive rocks, beginning with harzburgit up to two-mica granite.

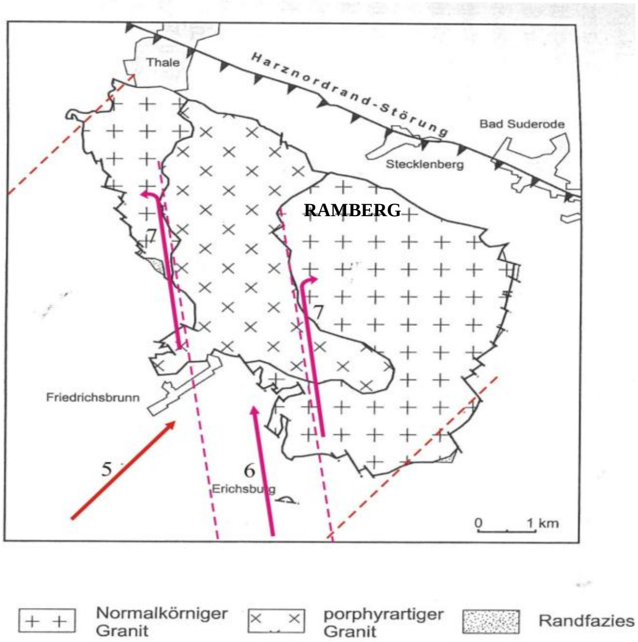

**Fig. 2:**

5. Introduction of Ramberg Massif in SW–NE (Rhine) direction;
6.Activation faults in the N-NW (Eggic) direction;
7. Flow of potassium and silicon fluids in the eastern and western part of the Ramberg.

The petrological-geochemical model of the formation of the igneous complex in the Harz Mountains based on the known geological-tectonic, geophysical and other fundamental facts of the geological structure and the spatial position of the Harz igneous rocks. The igneous formation in the Harz Mountains depends on the tectonic evolution in the Harz region. It is known that in the Rhenohercynian zone was an intense compression from southeast to northwest, which has led to the deformation of the crust and the formation of thrust faults, nappes and wedges. This is particularly evident in the Harz Mountains. As a result of tectonic processes a multiple granitisation in connection with the strong fluctuations of alkalinity-level of the liquid rock and migration of magamtic center was occurred.

In the formation of palingenetic rocks such special features for granitoids are characterized like the absence of batolites, the presence of closed-rounded plate shaped granitoids with a not deep base area (massif Brocken and Oker), which have no supply passages. Furthermore there is an abnormal crystallization-sequence for the rocks of the granitoid-series of palingenetic origin characteristically.

The acidification or “leaching” of the starting melt, which particularly occurs in the Brocken massif, may be explained with the formation of normal micro-pegmatite, drusy, porphyry-granites and also for the Ramberg massif with the formation of two-mica granites and quarz-mica rocks and the “hypothesis by the wave of acid components” and the theory of metasomatic zonality of Korjintskiy.

In the crystallization of the magmas, the ascending syn-magmatic and post-magmatic solutions with the movable acid-components are enriched, that does not act as components of the minerals. These components pass through more rapidly than the other components of the solution with the formation of the melt “upstream shaft“ of the acid components with an increased concentration. The acidity of the solutions is growing by leaps and bounds in the condensation and the corresponding compaction. In this phase, bases from the rocks are leached, which is simultaneously compensated by the deposition of quartz.

The leaching of the bases in the order of reducing the alkalinity, but also in connection with the general regularities of metasomatic zonality; that means that the small proportion of the base components is preferably removed from the rock. After reaching the maximum capacity of the acid inversion takes place.

After evaluating the petrological-geochemical data, the processes described above take place gradually after individual stages (Fig. 1–3): 1 – the peak of metamorphism is in the central German Crystalline zone, here is the regeneration of magmas; 2 – Rise of the andesite-basalt magma composition; 3 – The emplacement of the pluton and its ascent into the upper crustal parts; 4 – The position of the Brocken massif in the direction of the regional stress field; 5 – The cleavage of the Ocker massif in the area of the Acker-Bruchberg-mountain range.

I Stage (Figure 3, position 1 to 3) – There is in connection with the compression an partial melting of basaltic-andesito (toleiit) liquid rock and and the rise into the upper crustal part in direction of the Acker-Bruchberg-mountain range.

II Stage (Figure 3, position 4 and 5) – Due to the basalt melt the assimilation of crustal material is causing the formation of the Banatit-Granite-Series; this consists of rocks of the gabbro-diorite, diorite, quartz-diorite composition. It takes place the cleavage of the Ocker massif. The alkalinity level of the two stages corresponds to the alkalinity areas of I–V by Korjintskiy [Gevorkian R.G., Klisch I., 2009]. Geochemically predominates sodium prior potassium.

III Stage (Figure 1, position 3) – The cleavage of the Ilsenstein Massif takes place, it is the abrupt shift of the melt along the Variscan tectonic transition zone and along the east Avalonian crystallization foundation. Because of this intensive palingenetic processes proceed and it results in an increasing potassium alkalinity (microclinization). These processes lead to the formation and cleavage of the gabbro-harzburgite formationof the toleiit-basaltic melt with special features of increased alkalinity, these results in the formation of mica-peridotites.

IV Stage (Figure 1, position 4) – There is a further shift of the igneous masses along the Varis can sliding zone from northeast to southeast. The alkalinity of the melt increases further. It is interesting that the magmatic center along the line of contact of the Ilsenstein Massif has shifted towards the granodiorite zone and into contact with the micro-pegmatitegranite of the Brocken massif.

In micro-pegmatitegranite the spherolite-myrmekite clarifies the amplification of tectonic cataclasite related to the amplification of tectonic stresses and the tectonic deformation. The formation of spherolite-myrmekite is due to the increase in the activity of the fluids and the temperature increase in the contact zone [Gevorkian R.G., Klisch I., 2011]. The biotite schlieren are interpreted as the biotite-line which based on the diagram of the paragenesis of granitoid rocks of the Schreinemacker-projection – are represented by Korzinskiy.The lenticular slide textures at the hornblende-granites indicate the intense delivery of both potassium-components and quartz, which are necessary for the reaction processes of Area I to Area II to allow for Korzinskiy [Gevorkian R.G., Klisch I., 2009].

The processes described above point out the trachytic texture and the formation of hybrid rocks, such as the green and bright augite-granite. This results in a geochemically overhang potassium over sodium.

V Stage (Figure 1) – There is a further shift of the melt of the along the northern edge disturbance of the Harz Mountains and the assimilation of quartzite of the Acker-Bruchberg-mountain range which leads to acidification of the melt and reduce the low alkalinity. These processes lead to the peritectic translation along the cotectic crystallization-lenses of the melt from the Level IV to Level II according to Korzinskiy.

Petrological it results in the formation of blust-structures in fine-grained edge-granites, which are interpreted as rapid enrichment of quartz mobilisaten in interstices of minerals. Compared to drusy granites it took place, as described above, the increasing proportion of the quartz, while the Alkali feldspar proportion remains stable.

VI Stage (Figure 2, position 5 and 6) – with the rise of magma in the upper parts of the crust (Figure 3, position 3) is the placement of the stock-like Ramberg Massif of southeast to northeast in the Rhenohercynian direction.

In connection with the activation of faults in eggic direction (north-northwest), the cause of the change in tectonic stresses can be represented and take place in the gneiss formation processes on the rocks of the Ramberg Massif and it comes to the formation of two-mica granites and quartz-mica rocks.

The presented petrological-geochemical model shows the migration of the initial melt of the Harz Mountains from southeast to northwest, which has led in stages to changes in the composition of the melt, until the formation of granitoids based on the progressive palingenesis of igneous displacement and metasomatism [Gevorkian R.G., Klisch I., 2009].

References:

1. Gevorkian R.G., I. Klisch (2009). Geochemical percularity and petrogenesis of Harz (Germany) and Bazumo-Pambakskoy oblasti (Armenia) magmatic rocks. Yerevan: EDIT PRINT, 307 p.
2. Gevorkian R.G., I. Klisch (2011). Regularity of rocks granitization process of massif Brocken (Harz, Germany). Rus.Ann.Sem. Exp.Min.Petrol.Geochi. 2011, April 16-17 Abs. GEOKHI RAS, p.33-34 (in Russian).
3. Bachmann ssGerhard H., Bodo-Carlo Ehling, Rudolf Eichner und Max Schwab (2008). Geologie von Sachsen-Anhalt. Stuttgart: E. Schweizerbart'sche Verlagsbuchhandlung

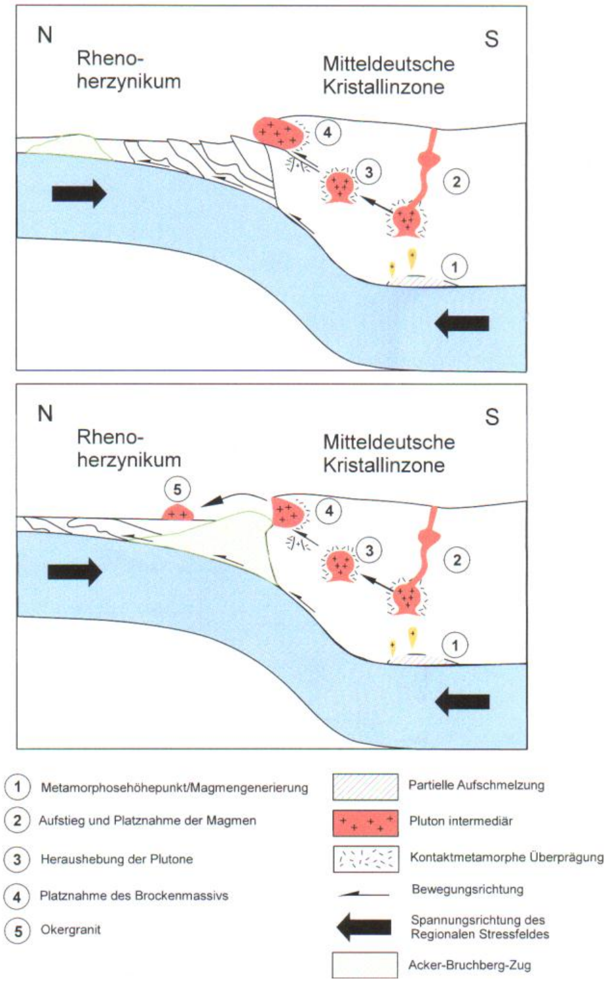

**Fig. 3**. A schematic model of the dynamic formation of Harz magmatism.

## Persikov E.S., Bukhtiyarov P.G. Viscosity of kimberlite and basaltic magmas during their ascent from mantle to the crust

Institute of experimental Mineralogy RAS, Chernogolovka

**Abstract.** Diamonds carrier kimberlite magmas will be ascent from mantle to the crust with the essential acceleration. This fundamental result has been established for the first time on the base of experimental and theoretical data [Persikov, 1991; Persikov, 1998; Persikov, Bukhtiyarov, 2004] using structural chemical model to predict the viscosity of magmatic melts [Persikov, 1998, 2007; Persikov, Bukhtiyarov, 2009]. Viscosity of kimberlite magmas will be decrease by 1.5 orders of magnitude during their evolution and the ascent from mantle to the crust in spite of considerable decreasing of the magmas temperature (about 550 °C), magmas partly degassing and crystallization during such process. On the contrary, the viscosity of basaltic magmas will be increase by about 2.0 orders of magnitude during their evolution and the ascent from mantle to the Earth crust.

*Key words: viscosity, kimberlite and basaltic magmas, temperature, pressure, model, melts*.

**Citation:** Persikov E.S., P.G. Bukhtiyarov (2013). Viscosity of kimberlite and basaltic magmas during their ascent from mantle to the crust. Vestn. Otd. nauk Zemle, RAN

We have experimentally proved that dependences of viscosity and activation energies of model aluminosilicate and magmatic melts on water and lithostatic pressures are inverse and extreme [Persikov, 1989, 1998; Persikov and Bukhtiyarov, 2004]. As an example, Fig. 1 and Fig. 2 show diagrams of dependences of viscosity and activation energy of viscous flow on lithostatic pressure for the melts of the system albite – dioside as well as for jadeite melt.

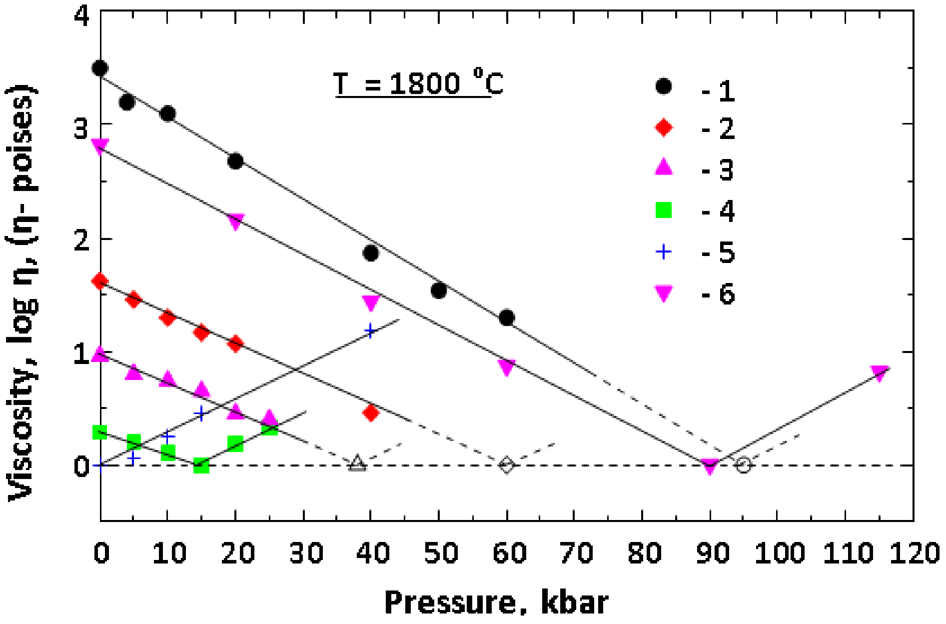

**Fig. 1.** Pressure dependence of the viscosity of model and magmatic melts at the isothermal condition.

1 - Ab100; 2 - Ab80Di20; 3 - Ab57Di43; 4 - Ab30Di70; 5 - Di100; 6 - Jd100 (filled symbols are based on the experimental data, the open ones are extrapolated values)

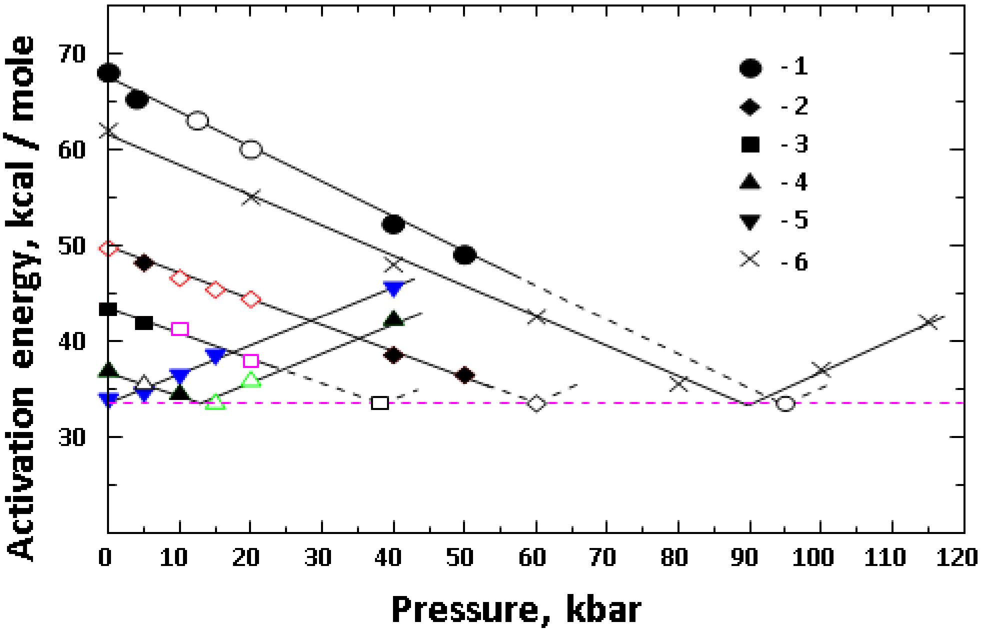

**Fig. 2**. Pressure dependence of the activation energy of a viscous flow of model and magmatic melts: system Ab-Di and Jd melts.
1- Ab100 ; 2 - Ab80Di20; 3 - Ab57Di43; 4 - Ab30Di70; 5 - Di100; 6 - Jd100 (open symbols are calculated values, melts composition in mol. %).

These results indicate that viscosity and activation energy markedly decrease with lithostatic pressure all over the compositional range from acid to basic (0 ≤ 100NBO/T < 200) and considerably increase after minimum points (for example, for tholleitic basalt with structural chemical parameter 100NBO/T = 80). But for diopside melt for which pressure dependences of viscosity and activation energy have the reverse character, i.e. the . We have experimentally established too the considerable effect of volume content of crystals and bubbles on viscosity of silicate and magmatic melts. As an example Fig. 3 gives our results of measurements of viscosity of the model system (silicon liquid + corundum crystals) [Persikov, Bukhtiyarov, 2004]. Analysis of these results shows that effective viscosity increases with the volume content of the crystalline phase (*Vcr.*). At *Vcr.* < viscosity and activation energy increase with pressure. An increase in viscosity and activation energy of both pyroxene and ultrabasic (200 < K < 400) melts, and more polymerized melts (0 < K < 200) after minimum points with pressure is in full agreement with the theoretical prediction [Persikov, Bukhtiyarov, 2004]. It should be noted that the value of 100NBO/T = 350 for kimberlite melts from pipe Udachnaya (Yakutiya), for example.

0.1 the dependence $\eta_{ef.} = f(Vcr.)$ is well approximated by the Einstein theoretical equation, but in the range 0.1 < *Vcr.* < 0.35 by the Einstein–Rosco empiric equation [Persikov, Bukhtiyarov, 2004]. However, at *Vcr.* > 0.35 the effect of the crystal content on the effective mixture viscosity is considerably larger (Fig. 3) and is approximated by the following empiric equation:

$$\eta_{эф.} = \eta_o(1 - Vкр.)^{-3.35} \qquad (1),$$

where $\eta_o$ is liquid phase viscosity. The Newtonian behavior of liquid has been observed at $Vcr. \leq 0.45$. At a further growth of crystal content the Newtonian behavior of liquid ($\tau_o = 0$) changed to the Bingham liquids with the limit of fluidity ($\tau_o$) is equal 2900 din/cm $^2$.

As for a separate effect of bubbles on the effective viscosity of the mixture, then the data obtained by us agree well with the results from [Uhira, 1980] and at $V_b \leq 0.45$ are described by the following empiric equation:

$$\eta_{эф.} = \eta_o(1 - V_{фл.})^{-0.55} \qquad (2),$$

where $V_b$ is a volume content of bubbles in the liquids.

Diamonds carrier kimberlite magmas will be ascent from mantle to the crust with the essential acceleration. This fundamental result has been established for the first time on the base of both ofmentioned above experimental data as well as on theoretical data [Persikov, 1991; Persikov, 1998; Persikov, Bukhtiyarov, 2004] using structural chemical model to predict the viscosity of magmatic melts [Persikov, 1998, 2007; Persikov, Bukhtiyarov, 2009]. Viscosity of kimberlite magmas will be decrease by 1.5 order of magnitude during their evolution and the ascent from mantle to the crust in spite of considerable decreasing of the magmas temperature (about 550 °C), magmas partly degassing and crystallization during such process. On the contrary, the viscosity of basaltic magmas will be.

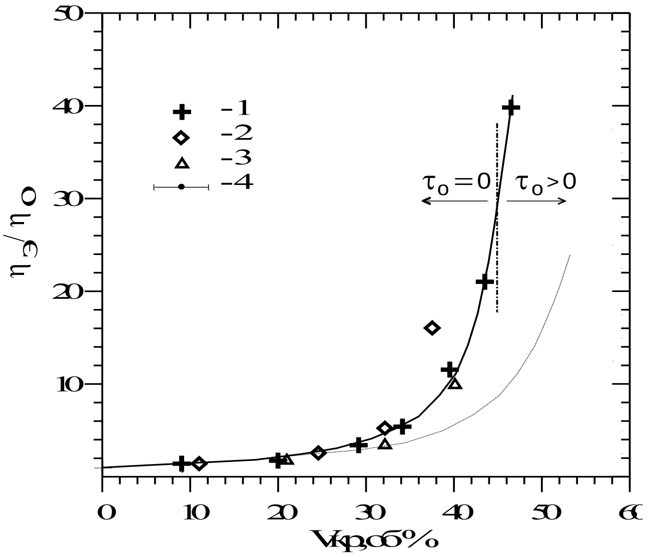

**Fig. 3.** Crystal content effect on the effective viscosity of the mixture (model heterogeneous melts)
1 - ηo = 3.8 Pa·s, crystals size 0.2 – 0.4 mm; 2 - $\eta_0$ = 0.68 Pa·s, crystals size 0.2 – 0.4 mm; 3 - ηo = 0.68 Pa·s, crystals size 0.16 – 0.2 mm; 4 - errors; dash line is consist to equation of Rosco

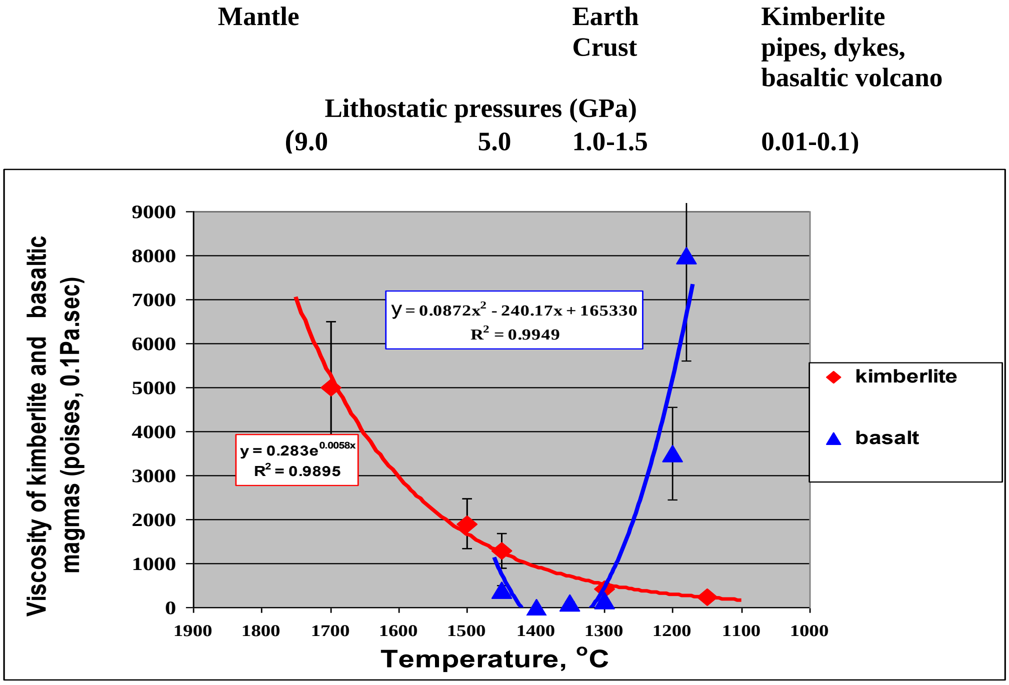

**Fig. 4.** Dynamics of viscosity of kimberlite and basaltic magmas during their ascent from mantle to the Earth crust

Kimberlite melts (100NBO/T ≈ 350) can be generated in mantle at small degrees of partial melting (0.1-0.7 vol. %) of carbonated peridotite at pressures up to 8-10 GPa or 80 – 100 kbar, (depths ≈ 250-340 km), temperature ≈ 1700 $^{o}$C and volume content of crystals ≈ 10 %. Viscosity of such melts will be high enough (≈ 5000 poises or 500 Pa·s) at these parameters (Fig.4). Results obtained indicated that viscosity of near – surface kimberlite melts will be much more lower during formation of kimberlite pipes, dykes and intrusions (≈ 250 poises or 25 Pa·s at pressures 50 –100 MPa, temperature ≈ 1150$^{o}$C and a volume content of crystals ≈ 40 %, Fig. 4). On the contrary, the viscosity of basaltic magmas (100NBO/T = 80) will be relatively small during generation in the mantle (≈ 400 poises or 40 Pa·s at the pressures up to 4-5 GPa, temperature ≈ 1450$^{o}$C and volume content of crystals ≈ 5 vol. %). Viscosity of ascending basaltic magmas will have minimum values at intermediate parameters (≈ 10 poises or 1 Pa·s at pressures 2-3 GPa, temperature ≈ 1350-1400 $^{o}$C and a volume content of crystals ≈ 10 %, Fig. 1, 2). Viscosity of basaltic magma at the final stage during volcanic eruption will be considerable increase (≈ 8000 poises or 800 Pa·s at pressures 0.1-10 MPa, temperature ≈ 1150$^{o}$C and a volume content of crystals ≈ 15 %, Fig. 4). It should be note that a lower viscosity of basaltic magmas to compare with kimberlite magmas at intermediate parameters (P = 1-3 GPa, T = 1300 $^{o}$C-1400 $^{o}$C ) can be explain by different volume content of crystals in these magmas (≈ 10 vol. % in basaltic magma and ≈ (20 – 35) vol. % in kimberlite magmas, Fig. 3).

---

This study was supported by RFBR, grant No 12-05-00164

References:

1. Persikov E.S. (1991). The viscosity of magmatic liquids: experiment, generalized patterns; a model for calculation and prediction; application. In: *Physical chemistry of magmas. Adv. Phys. Geochem*. L.L. Perchuk & I. Kushiro Eds. Springer-Verlag. New York., Vol. 9, P. 1-40.
2. Persikov E.S. (1998). The viscosity of model and magmatic melts under P-T-parameters of the Earth's crustand upper mantle. *Russian Geology and Geophysics*, V. 39, P. 1780-1792.
3. Persikov E.S., P.G. Bukhtiyarov (2004). Experimental study of the effect of lithostatic and aqueous pressures on viscosity of silicate and magmatic melts. A new structural-chemical model to calculate and predict the viscosity of such melts. In: *Experimental Mineralogy. Some Results on the Verge of a New Century*. Zharikov V.A., Fedkin V.V. (Eds.). Nauka, Moscow, Vol. 1, P. 103–122 (in Russian).
4. Persikov E.S. (2007). Structural chemical model to calculate and predict the viscosity of magmatic melts in full range of compositions and conditions. *General Assembly EGU-2007. Vienna. Geophysical Research. Abstracts*, Vol.9, A-02262, SRef-ID: 1607-7962/gra/EGU2007-A-02262C. European Geosciences Union.
5. Persikov E.S., P.G. Bukhtiyarov (2009). Interrelated structural chemical model to predict and calculate viscosity of magmatic melts and water diffusion in a wide range of compositions and T-P parameters of the Earth’s crust and upper mantle. *Russian Geology and Geophysics*, Vol. 50, No 12, P. 1-12
6. Uhira K. (1980). Experimental study on the effect of bubble concentration on the effective viscosity of liquids. *Bull. Earth Res. Inst.*, Vol. 56, P. 857-871.

---

## Persikov E.S., Bukhtiyarov P.G. Peculiarities of carbonates (calcite, dolomite) melting under pressures of different fluid composition (system C–O–H–Ar)

Institute of experimental Mineralogy RAS, Chernogolovka

**Abstract.** Melting experiments on calcite and dolomite at 100 MPa fluid (Ar, Ar + $H_2O$, $CO_2$, $CO_2$+$H_2O$) pressures were carry out in the temperature range 550 $^{o}$C – 1330 $^{o}$C. These parameters are corresponded to the conditions of kimberlite pipes and dykes formation. A unique high gas pressure apparatus [Persikov, 1991; Persikov, Bukhtiyarov, 2002] has been used for experiments in which the mass balance control in each run has been done. The mechanism of the formation of carbonatite melts at low temperatures (≤ 1100 $^{o}$C) under water bearing fluid pressures was proposed. These temperatures are considerably lower of the calcite incongruent melting temperature (1320 ± 10 $^{o}$C) which has been experimentally obtained.

*Key words: melting, calcite, dolomite, temperature, pressure, fluid, mechanism, water,* melts.

**Citation:** E.S. Persikov, P.G. Bukhtiyarov (2013). Peculiarities of carbonates (calcite, dolomite) melting under pressures of different fluid composition (system C–O–H–Ar). Vestn. Otd. nauk Zemle, RAN …

Melting experiments on calcite and dolomite at 100 MPa fluid (Ar, Ar + $H_2O$, $CO_2$, $CO_2$+$H_2O$) pressures were carry out in the temperature range 550 $^{o}$C – 1330 $^{o}$C using a unique high gas pressure apparatus [Persikov, 1991; Persikov, Bukhtiyarov, 2002]. The apparatus involves internally heating high pressure vessel (IHPV). The IHPV is equipped with original internal device which is now modernized [Persikov, Bukhtiyarov, 2002]. This study has been done to understand of the effects of high lithostatic and water bearing fluid pressures on mechanisms of the melting of calcite and dolomite. The character features of this study which is differ from known enough experimental and theoretical results on melting and a phase relations in fluid bearing carbonate systems [Wyllie, Tuttle, 1960; Wyllie, 1965; Irving and Wyllie, 1975; Huang and Wyllie, 1976; Treiman 1995; and some others] are as follows. The dependence of carbonates melting mechanisms on small water content in Ar or $CO_2$ fluids at high pressures has been established for the first time.

Calcite incongruent melted at T = 1320$^{o}$ ± 10$^{o}$C under water free Ar or $CO_2$ pressures (modeled the lithostatic pressures) releasing 5.27 wt. % $CO_2$ in the fluid (see table 1) and formed of carbonatite melt. The composition of this melt (92.3Cal + 7.7CaO, wt. %) has been obtained using the results of the mass balance control which was done for each experimental run. Both calcite and association of CaO + $CaCO_3$ have been determined in quenched samples by microprobe analyses. These results are consistent both to theoretical value of the temperature of calcite incongruent melting at 100 MPa $CO_2$ pressures [Treiman, 1995] and with the experimentally determined bracket for calcite incongruent melting (1300$^{o}$ – 1320$^{o}$C) established early [Huang and Wyllie, 1976; Irving and Wyllie, 1975].

Dolomite is partly decomposed into calcite + periclase + $CO_2$ at the T > 800 $^{o}$C (table 1) and the calcite formed is incongruent melted at the T = 1320 $^{o}$C, releasing much $CO_2$ in sum (26.9 wt. %). Both periclase and association of CaO + $CaCO_3$ have been determined in quenched samples by microprobe analyses. This result is consistent to the suggested reaction *(1)* of dolomite partial melting:

$$MgCa(CO_3)_2 = MgO + 0.88CaCO_3 + 1.12CO_2 \qquad (1)$$

solid solid melt fluid

A complete another result has been obtained in the runs with a small amount of water (up to 3 wt. %) in $CO_2$ or Ar fluids. In these cases the calcite crystals begin melting at the 1100 °C (sample No 1, table 1) and melted in full at moderate temperature showed at the table 1. The $CO_2$ loss from samples at high temperatures was about 13 wt. % (samples No 13 and 14). Portlandite - $Ca(OH)_2$, calcite and association of (Prd + Cal) have been determined in quenched samples using microprobe analyses. It should be noted that the simple incongruent melting of calcite can't explain such full melting because the $CO_2$ loss should be just 5.27 wt. % for such melting. Based on data obtained and the results of mass balance calculations as well as on experimental data on melting in the system portlandite – calcite [Wyllie, Tuttle, 1960; Wyllie, 1965] the following mechanism has been proposed.

The calcite reacts with a water-bearing fluid to form portlandite at temperatures up to 680 °C by the reaction $CaCO_3 + H_2O = (Ca(OH)_2 + CO_2$. Portlandite formed in this reaction reacts with calcite resulting in the form of a eutectic melt (56Prd + 44Cal, вес. %) + solid Cal in the temperatures range 680° – 1100 °C. At temperatures higher than 1100 °C this system should be completely molten. The composition of formed carbonatite melt ((25.5Prd + 74.5Cal, wt.. %) as well as the $CO_2$ loss on such melting (13.14 wt. %) have been obtained using the mass-balance calculations. This result is consistent to the suggested reaction *(2)* of calcite melting under water-impoverished fluid pressures:

$$CaCO_3 + 0.316H_2O = 0.316Ca(OH)_2 + 0.684CaCO_3 + 0.316CO_2$$

solid fluid melt fluid (2)

**Table 1.** Experimental conditions and some results for the melting of the calcite and dolomite at $P_{fl}$ = 100 MPa

| Runs number | T °C | Fluid composition (wt. %); oxygen buffer* | The scheme of Pt capsules with samples | | Run duration (min) | Weight losses after run ($CO_2$, wt. %) |
|---|---|---|---|---|---|---|
| | | | **before run** | **after run** | | |
| 2a | 1320 | Ar, $CO_2$<br>Mo-$Mo_2O_3$ | 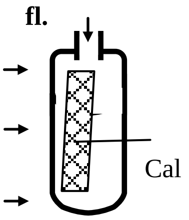 | 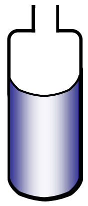 | 30 | 5.25<br>5.27 (calculated) |
| 1 | 1100 | 97Ar + $3H_2O$; HM | | | 15 | 12.7<br>13.1 (calculated) |
| 14 | 1260 | 97Ar + $3H_2O$; HM | | | 120 | 12.8<br>13.1 (calculated) |
| 13 | 1280-top<br>1300- bottom | $98CO_2 + 2H_2O$;<br>HM | | | 120 | 13.1<br>13.1 (calculated ) |
| 2b | 1310 | Ar, $CO_2$<br>Mo-$Mo_2O_3$ | 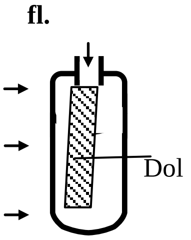 | | 30 | 26.9<br>26.8 (calculated) |
| 15 | 1260 | 97Ar + $3H_2O$; HM | | 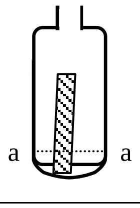 | 120 | 30.4<br>30.5(calculated) |
| 3 | 1280- top<br>1300- bottom | $98CO_2 + 2H_2O$;<br>HM | | | 120 | 31.5<br>30.5(calculated) |

Abbreviations: HM – is the hematite/magnetite buffer

The dolomite (samples No 3 and No 15, table 1) are partly decomposed under water- impoverished fluid pressures at temperatures T ≤ 530 °C to form (Per) - MgO, $CO_2$ and calcite which is melted at higher temperatures by mentioned above mechanism. The $CO_2$ loss on such melting was 30.5 wt. % is not consistent of the full decomposed reaction of dolomite (47.72 wt.. % $CO_2$) but consistent to the suggested reaction *(3)* of partial dolomite melting under water- impoverished fluid pressures:

$$MgCa(CO_3)_2 + 0.316H_2O =$$

solid fluid

$$=MgO + 0.316Ca(OH)_2 + 0.684CaCO_3 + 1.316CO_2 \qquad (3)$$

solid melt fluid

The low density and low viscosity melt formed is mostly separated from dolomite and collected at the bottom of the Pt capsule and formed a differentiated crust around a mostly periclase core (table 1). Using microprobe analyses we found mostly periclase and a small amount of calcite in a periclase-rich restile and both calcite and the association of CaO + calcite in formed melt as the crust of this sample. It is interesting that the all admixture elements of dolomite such as $Al_2O_3$, $SiO_2$, $P_2O_5$ are separated to the external surface of differentiated melt (table 1)

---

This study was supported by RFBR, grant No 12-05-00164 and by the program No 9 of the BGS RAS

References:

1. Huang W.L. and P.J. Wyllie (1976). Melting relationships in the system CaO - CO2 and MgO - CO2 to 33 kilobars. Geoch. et Cosmoch. Acta, V. 40, P. 129-132
2. Irving A. J. and P.J. Wyllie (1975). Solidus and melting relationships for calcite, magnesite, and the join CaCO3 - MgCO3 to 36 kilobars. Geoch. et Cosmoch. Acta, V. 39, P. 35-53.

3. Persikov E.S. (1991). The viscosity of magmatic liquids: experiments, generalized patterns. A model for calculation and prediction. Applications. In "*Physical chemistry of magmas. Advances in Physical Geochemistry*", L.L. Perchuk, and I. Kushiro, eds., Springer-Verlag, V. 9, P. 1-40.
4. Persikov E.S., P.G. Bukhtiyarov (2002). Unique gas high pressure apparatus to study fluid - melts and fluid - solid - melts interaction with any fluid composition at the temperature up to 1400 $^oC$ and at the pressures up to 5 kbars. *J. Conf. Abs.*, V. 7, No 1, P. 85.
5. Treiman A.H. (1995). Ca-rich carbonate melts: A regular-solution model, with applications to carbonatite magma + vapor equilibria and carbonate lavas on Venus. *Amer. Mineral.*, V. 80, P. 115-130.
6. Wyllie P.J., O.F.Tuttle (1960). The system $CaO-CO_2-H_2O$ and the origin of carbonatites *J. Petrology,* V. 1, P. 1-46
7. Wyllie P.J. (1965). Melting relationships in the system $CaO-MgO-CO_2-H_2O$, with petrological applications. *J. Petrology,* V. 6, P. 101-123.

## Chevychelov V.Yu. The effect of $CO_2$ on the solubility of $H_2O$-Cl fluids in dacitic melt. The first experimental results

Institute of Experimental Mineralogy RAS, Chernogolovka

**Abstract.** The solubility of $H_2O-CO_2$-Cl-containing fluids in dacitic melt is experimentally studied at $T$=1000°C, $P$=200 MPa and log$f_{O2}$ ~(Ni-NiO)+3.5. The obtained results are compared with data from similar experiments in the system with rhyodacitic melt and $H_2O$-Cl-containing fluids without $CO_2$. The Cl content in the melt in system with $CO_2$ is higher than in the system without $CO_2$ at the mole fraction of Cl in fluid > 0.03-0.06. The addition of $CO_2$ to the system has influence with the $H_2O$ content in dacitic melt, in this case the water content of the melt decreases by about 0.5-1.0 wt.%.

*Key words: dacitic melt, fluid, $CO_2$, $H_2O$, Cl, solubility, experiment.*

**Citation:** Chevychelov V.Yu. (2013) The effect of $CO_2$ on the solubility of $H_2O$-Cl fluids in dacitic melt. The first experimental results. *Vestnik Otdelenia nauk o Zemle RAN*

A release of volatiles from magmas, commonly associated with the pressure drop and melt crystallization, accompanied by magma ascent from crustal depths and by magmatic eruptions and may be a driving force for these processes. In this regard $CO_2$ formed during assimilation carbonate rocks by melt may have a significant effect on the solubility of other volatiles (e.g., Cl) in magma [Dallai et al., 2011]. At the present time these processes are poorly studied [Botcharnikov et al., 2007]. Melts of intermediate composition such as dacitic melt characterized by higher solubility $CO_2$ in comparison with rhyolitic (predominance molecular $CO_2$) or basaltic (dominant carbonate form) composition due to the fact that they contain both types of species. The ratio of $CO_2$mol/carbonate in the quenched glasses strongly decreases with increasing water content in dacitic melt [Behrens et al., 2004; Botcharnikov et al., 2005; Holloway, Blank, 1994; Tamic et al., 2001].

Solubility $H_2O-CO_2$-Cl-containing fluids of various concentrations in synthetic dacitic melt (Table 1) is experimentally studied at T=1000$^o$C, P=200MPa and logf$_{O2}$ ~(Ni-NiO)+3.5. Chlorine is initially introduced into the system as aqueous HCl solutions of varying concentration, and $CO_2$ is introduced as ethane diacid $H_2C_2O_4 \times 2H_2O$ plus hydrogen peroxide $H_2O_2$. Five mg of an aqueous solution, one – one and half mg of ethane diacid and fifty mg of synthetic dacitic glass powder, obtained in preliminary experiments, were loaded in Pt capsules. Experiments are carried out in a internally heated pressure vessel (IHPV). The duration of the runs was 5 days.

After the experiments the content of gaseous $CO_2$ in the capsule was measured by a conventional weight-loss method (the capsule was frozen in liquid nitrogen, then it pierced by a needle, and it heated to room temperature). The content of $H_2O$-Cl components in the solution was measured in the same way (the capsule, punctured by needle, heated at 110$^o$C for 3 minutes). The quenched glasses composition and the Cl content of the quenched glasses were analyzed with electron microprobe. After the experiments the visible crystallization in the quenched glasses were not found. Unfortunately, the $CO_2$ content in the quenched glasses is not currently analyzed. The $H_2O$ content in the quenched glasses is determined by KFT, by «by-difference» and by mass balance methods. The composition of the $H_2O-Cl-CO_2$ fluid was constrained from mass balance, knowing the initial and final amounts of fluid components and the final concentrations of $H_2O$ and Cl in the glasses. More detailed the methodology for realization of the similar experiments and the analysis conditions of quenched phases are described in [Chevychelov et al., 2008].

**Table 1.** Chemical compositions (wt.%) of synthetic dacitic and rhyodacitic melts

| The melt composition | $SiO_2$ | $TiO_2$ | $Al_2O_3$ | $FeO_{tot}$ | MgO | CaO | $Na_2O$ | $K_2O$ | A/CNK |
|---|---|---|---|---|---|---|---|---|---|
| Dacitic ($H_2O-CO_2$-HCl -fluid) | 67.0 | 0.6 | 16.6 | 4.1 | 1.4 | 3.5 | 4.0 | 2.7 | 1.05 |
| Rhyodacitic ($H_2O$-HCl -fluid) | 70.1 | 0.5 | 14.2 | 3.6 | 1.4 | 4.1 | 3.2 | 2.8 | 0.90 |

The obtained results are compared with those from similar experiments with rhyodacitic melt (Table 1) and $H_2O$-Cl-containing fluids without $CO_2$ [Chevychelov, 2013]. At low Cl content in the system the $CO_2$ content in the system has no appreciable effect on the Cl content in the melt. The Cl content in the melt in system with $CO_2$ is higher than in the system without $CO_2$ at the mole fraction of Cl in fluid > 0.03-0.06 (Fig. 1). It can be assumed that the activity coefficient of Cl in the fluid could increase with addition of $CO_2$, causing an increase in Cl content in the melt.

The addition of $CO_2$ to the system also has a significant influence on the $H_2O$ content in dacitic melt, in this case the water content of the melt decreases by about 0.5-1.0 wt.% (Fig. 2). This effect is probably related to the dilution of the fluid by carbon dioxide resulting in the mole fraction of $H_2O$ and the fugacity of $H_2O$ in the fluid decrease.

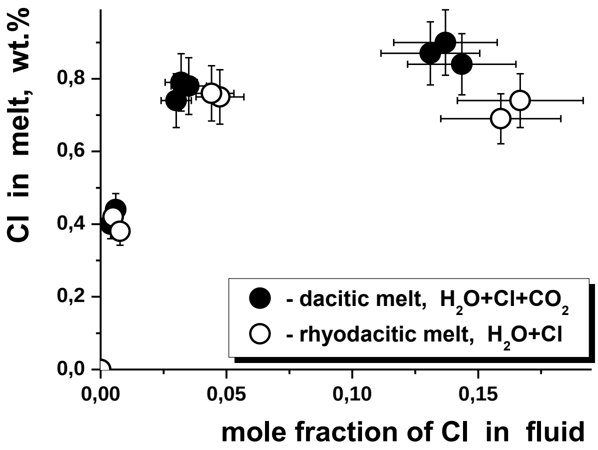

**Fig. 1.** Dependence of the Cl content in the dacitic (rhyodacitic) melt on the total Cl content in the coexisting fluid. Effect of the $CO_2$ addition.

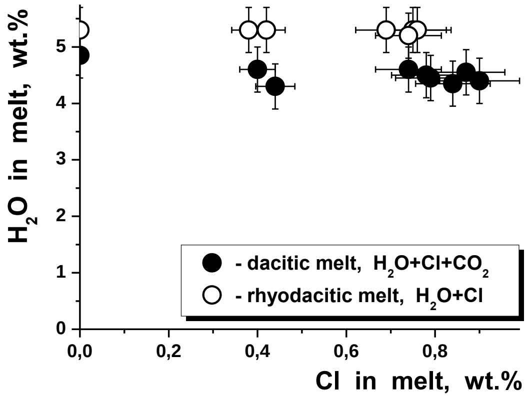

**Fig. 2**. $H_2O$ content and Cl content in dacitic (rhyodacitic) melt as well in $CO_2$-containing system as in a system without $CO_2$.

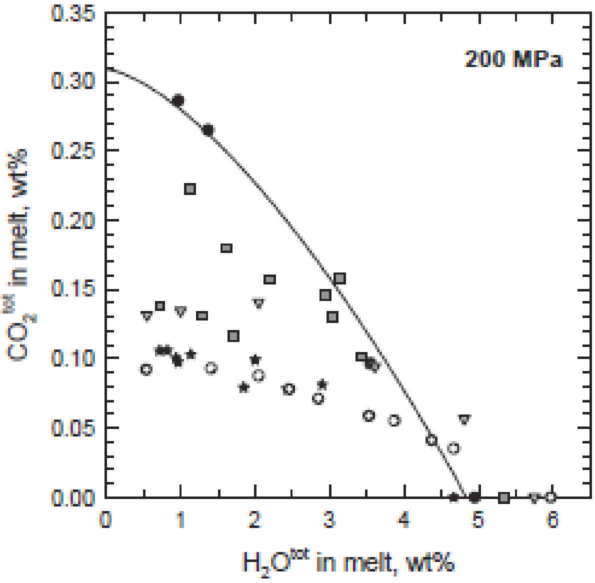

**Fig. 3.** The contents of $H_2O$ and $CO_2$ in various magmatic melts: rhyolitic (white circle), dacitic (triangle), andesitic (square), tholeiitic (asterisk) and phono-tephritic (black circle). The figure is taken from the paper [Behrens et al., 2009].

Our experiments were carried out at relatively low $CO_2$ content in approaching to water-saturated conditions for dacitic melt. At lower $H_2O$ content and not water-saturated melts the solubility of $CO_2$ in the phases of the system and the effect of $CO_2$ on the behavior of other volatiles can significantly increase (Fig. 3) [Botcharnikov et al., 2007].

---

This work was supported by RFBR grant № 11-05-00991-a.

References:

1. Chevychelov V.Yu. (2013). Partitioning of volatiles, rock-forming and ore components in magmatic systems: experimental studies. *Author's abstract ... Doctor of Science.* Moscow, 64 p.
2. Behrens H., S. Ohlhorst, F. Holtz, M. Champenois (2004). $CO_2$ solubility in dacitic melts equilibrated with $H_2O$-$CO_2$ fluids: Implications for modeling the solubility of $CO_2$ in silicic melts. *Geochim. Cosmochim. Acta,* V. 68, No 22, P.4687-4703.
3. Behrens H., V. Misiti, C. Freda, F. Vetere, R.E. Botcharnikov, P. Scarlato (2009). Solubility of $H_2O$ and $CO_2$ in ultrapotassic melts at 1200 and 1250°C and pressure from 50 to 500 MPa. *Am. Mineral.,* V. 94, P.105-120.
4. Botcharnikov R., M. Freise, F. Holtz, H. Behrens (2005). Solubility of C-O-H mixtures in natural melts: new experimental data and application range of recent models. *Annals of Geophysics.,* V. 48, No 4/5, P.633-646.
5. Botcharnikov R.E., F. Holtz, H. Behrens (2007). The effect of $CO_2$ on the solubility of $H_2O$-Cl fluids in andesitic melt. *Eur. J. Mineral.,* V. 19, P.671-680.
6. Chevychelov V.Yu., R.E. Botcharnikov, F. Holtz (2008). Partitioning of Cl and F between fluid and hydrous phonolitic melt of Mt. Vesuvius at ~850-1000°C and 200 MPa. *Chem. Geol.,* V. 256, No 3-4, P.172-184.
7. Dallai L., R. Cioni, C. Boschi, C. D'Oriano (2011). Carbonate-derived $CO_2$ purging magma at depth: Influence on the eruptive activity of Somma-Vesuvius, Italy. *Earth Planet. Sci. Lett.,* V. 310, No 1-2, P.84-95.
8. Holloway J.R., J.G. Blank (1994). Application of experimental results to C-O-H species in natural melts. *Rev. Mineral.,* V. 30, P.187-230.
9. Tamic N., H. Behrens, F. Holtz (2001). The solubility of $H_2O$ and $CO_2$ in rhyolitic melts in equilibrium with a mixed $CO_2$-$H_2O$ fluid phase. *Chem. Geol.,* V. 174, P.333-347.

---

## Aksyuk A.M., Korzhinskaya V.S., Konyshev A.A. Experimental study melting tourmaline granite from Komsomol'sk area in HF-$H_2O$ fluid

Institute of Experimental Mineralogy RAS, Chernogolovka

**Abstract**. Formation of large Sn deposits on Komsomolsk area, (the Far East of Russia), are connected with tourmaline granites. Experimental researches of P-T parameters for granite from the Solnechnoe deposit are made under pressure of 0.5-2 kbar in the water, and 0.1 m HF. Solidus parameters for tourmaline granite were close to solidus of gaplogranite.

*Key words: experiment, tourmaline granites, melting, Komsomolsk area.*

**Citation**: Aksyuk A.M., V.S. Korzhinskaya, A.A. Konyshev (2013). Experimental study melting tourmaline granites from Komsomol'sk area in HF-$H_2O$ fluids. Bulletin ONZ RAS, (doi:

Formation of the large Sn deposits on Komsomolsk area, (the Far East of Russia), are connected with tourmaline granites. Evaluation of fluorine concentrations in natural granite fluid, took part in the formation of the granites and tin-bearing deposits, were obtained on the basis of the published data on compositions of micas from the granites of the Komsomolsk ore-magmatic systems [Gonevchuk, 2002] and the equations of experimentally calibrated mineral geofluorimeters [Aksyuk, 2002, 2009]. The HF concentrations are presented in Fig. 1.

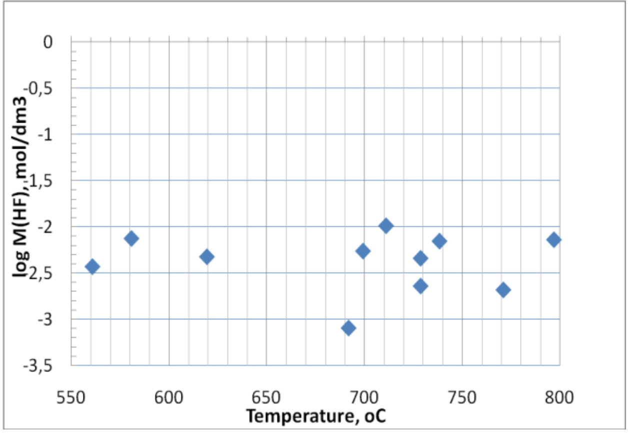

**Fig. 1** Concentration of HF (M, mole/dm$^3$) in fluids of tourmaline granites for the Komsomolsky area, defined with the help of biotite geofluorimeters [Aksyuk, 2002]

It can be seen that the volumetric concentrations of fluoride in fluid were in the range of 0.01-0.003 M (mol/dm$^3$), which corresponds to the depth of formation of granite at depths of 4 km, where the pressure is about 1 kbar, that is m(HF) (mol/kg $H_2O$) of about 0.01-0.04.

According to our estimates the biotite from granite of the Solnechnoe deposit formed at temperature of about 740°C. Concentration of HF in fluid equilibrium with that was supposed to be about 0.007 mol/dm$^3$, which seems quite typical and realistic to the Komsomolsk area. Comparison of concentrations of HF in the natural fluids, took part in the formation of biotite from tourmaline granite, developed in the Komsomolsk area, with similar estimates obtained by us for mica from other regions and fields (Eastern Transbaikalia and Primorye - Ta-Nb deposits; or from the Central Kazakhstan (Акчатау - W-Mo deposits) [Aksyuk, 2002, 2009], shows that the development of tourmaline granite and Sn deposits of Komsomolsky district held at relatively low fluoride concentration in fluid. Such a mode of fluorine is more characteristic for barren granites of the Kazakhstan and leucogranite of the Urals, or porphyry copper deposits of Baikal area, for which, in the opinion of the V.I. Sotnikov, A.N. Berzina and other researchers, apparently, was more characteristic chloride fluid. The Komsomolsk tin ore-magmatic system is one of the most thoroughly studied in geological respect [Gonevchuk, 2002]. The content of boron and fluorine in granites are often correlated with high content of tin, so it is important to evaluate the impact of the fluid components for melting of tourmaline granite experimentally. The experiments were performed in the IEM RAS at high temperatures (650-800°C) and pressures (0.5-2 kbar).

The experiments to study the solidus were carried out at hydrothermal facilities of high pressure with powders of natural tourmaline granite of the tin Solnechnoe deposit in the Komsomolsk ore region. Samples of rock were kindly made available to us by N.V. Gorelikova (IGEM RAS). P-T position of tourmaline granite solidus in the experiment was determined by the appearance of the first traces of glass in e experiment products, defined with the help of optical and electron microscope. As a result of the conducted experiments were first obtained the experimental evaluation of P-T parameters of the start melting tourmaline containing tinny granites for the Komsomolsk area (the Far East, Russia). As a result for the first time were obtained P-T parameters of the start melting the tourmaline containing tin-bearing granites of the Komsomolsk district in water and water-fluoride fluid (0.1 m HF) (Fig. 2).

The results clearly show that solidus of tourmaline granite from the Solnechnoe Sn deposit in the water, and 0.1 m HF close to T-P parameters to gaplogranite solidus at a pressure of up to 2.0 kbar. According to preliminary experiments at higher pressure it begins to deviate in a more low-temperature area that requires additional research.

Acknowledgements: The work was done with the financial support of the ONZ-2 Program.

References:

1. Aksyuk A.M. (2002). Experimentally calibrated geofluorimeters and mode of fluoride in granite fluids. *Petrology*, V. 10, n 6, pp. 628-642 (in Russian).
2. Aksyuk A.M. (2009). Mode of fluorine in deep sea hydrothermal fluids and near-surface waters. The author's abstract of doctoral dissertation. Moscow, 59 p. (in Russian).
3. Gonevchuk V.G. (2002). Tin-bearing systems of the Far East: Magmatism and formation of ore mineralization. Dalnauka. Vladivostok, 275 p. (in Russian).

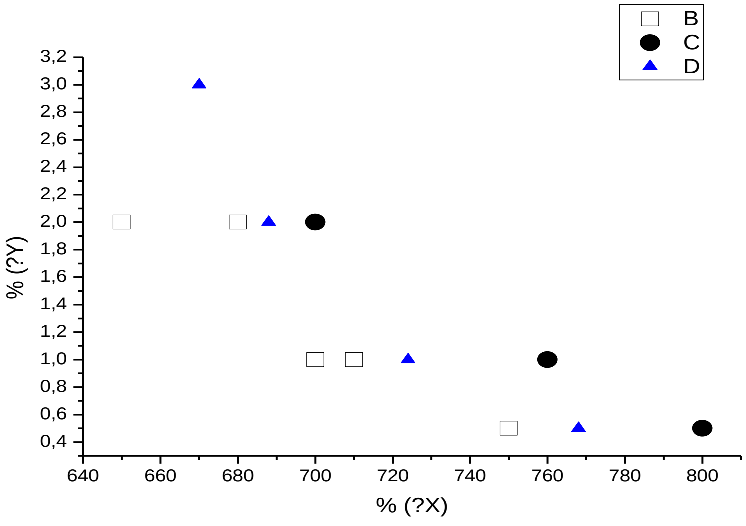

**Fig. 2.** Solidus of tourmaline granite of Komsomolsk district, in the water, and 0.1 m HF.It is close to T-P parameters for gaplogranite solidus

# Kadik A.A., Kryukova E.B., Koltashev V.V., Tsekhonya T.I. Solubility of reduced N-C-O-H volatiles in Fe-bearing silicate melts at high pressure and temperature and low oxygen fugacity

V. I. Vernadsky Institute of Geochemistry and Analytical Chemistry RAS, Moscow
Fiber Optics Research Center RAS, Moscow

**Abstract.** In the present paper we will focus on solubility of reduced N–C–H–O volatiles in iron-bearing silicate melts at high pressure 4 GPa and temperature 1550 °C, and low fO2 values 3.2 log units below iron–wüstite (IW) buffer equilibrium, i.e. $fO_2$=IW-3.2. To elucidate the mechanisms of N, C, O и H mutual solution in magmas and quantify the abundance of their species as a function of $fO_2$, we studied the glasses produced by quenching the model reduced silicate melts ($FeO–Na_2O–Al_2O_3–SiO_2$) using Infrared (IR) Fourier and Raman spectroscopies.

*Key words: N-C-O-H volatiles, magma ocean, Raman and IR spectroscopy, hydroxyl, molecular $H_2O$, oxygen fugacity.*

**Citation:** Kadik, E.B. Kryukova, V.V. Koltashev, T.I. Tsekhonya (2013). Solubility of reduced N-C-O-H volatiles in Fe-bearing silicate melts at high pressure and temperature and low oxygen fugacity

The large-scale melting of the early Earth should have been accompanied by a formation of volatile species, which composition was controlled by interaction of the main gas-forming C–N–H–O elements with silicate and metallic melts at low oxygen fugacity ($fO_2$) values prevailing during metal segregation and self-oxidation of magma ocean. Solubility of volatiles in magmatic melts strongly depends on pressure, temperature, composition, and $fO_2$. In the present paper we will focus on solubility of reduced N–C–H–O volatiles in iron-bearing silicate melts at high pressure 4 GPa and temperature 1550 °C, and low $fO_2$ values 3.2 log units below iron–wüstite (IW) buffer equilibrium, i.e. $fO_2$=IW-3.2.

To elucidate the mechanisms of N, C, O и H mutual solution in magmas and quantify the abundance of their species as a function of $fO_2$, we studied the glasses produced by quenching the model reduced silicate melts ($FeO–Na_2O–Al_2O_3–SiO_2$) using Infrared (IR) Fourier and Raman spectroscopies in a manner similar to that reported by [Kadik et al., 2004, Javoy et al., 2010]. Typical measurement results are shown in Figs.1 и 2, respectively. Experiments indicate that silicate melts contain the species with N–H bonds ($NH_3$, $NH^{4+}$, $NH^{2-}$) C–H bonds ($CH_4$), $H_2$ and $N_2$ molecules, and oxidized H species ($OH^-$ and $H_2O$) (Fig. 1, 2). In $fO_2$ region from IW-2 to IW-5 the solubility of N, C and H ranges from 0.4 to 1.9 wt.%, 0.4 and 0.3 wt.%, 0.2 and 0.3 wt.%, accordingly.

As is seen from Fig.1, the position and shape of a wide asymmetric absorption band at 3548 $cm^{-1}$ corresponds to stretching vibrations of hydroxyl groups $OH^-$ and molecules $H_2O$ [Newman, et al., 1986, Kadik et al., 2004]. A sharp peak at 1632 $cm^{-1}$ is a result of deformational (bending) vibrations of molecules $H_2O$ [Dianov et al., 2005]. In both peaks a reduction of their intensity is observed with lowering $fO_2$ within the values of $\Delta \log fO_2$ (IW) from -2 to -4, so the content of oxidized hydrogen forms $OH^-$ and $H_2O$ decreases in glasses.

The absorption coefficient α of studied glasses has been calculated from thus obtained IR absorption spectra from the 3548 $cm^{-1}$ and 1632 $cm^{-1}$ bands corresponding to vibrations of hydroxyl groups $OH^-$ and $H_2O$ molecules. To calculate the extinction coefficient ε thereof we have used its empirical dependence on the structural parameter NBO/T obtained in [Mercier et al., 2010]. After all the $OH^-$ and $H_2O$ contents in glasses are calculated using the Lambert-Beer law [Stolper, 1982]: $C = \alpha \times 18.02 / \rho \times \varepsilon$. Hydroxyl $OH^-$ content has made 4.58 wt.% in the IR band at 3548 $cm^{-1}$, and the content of $H_2O$ molecules dissolved in glass amounted to 1.63 wt.%. at 1632 $cm^{-1}$.

The initial Raman spectrum was decomposed into Gaussian components to identify volatile species. The spectra were normalized to a band around 490 $cm^{-1}$ (the fundamental vibration in pure $SiO_2$ glass). Results of decomposition are given in Fig. 3.

Due to correlation in intensity the bands can be grouped as follows:

- a band with a maximum at 3550-3570 $cm^{-1}$ ($OH^-$-groups in pure silica glass), the intensity of the band grows with $fO_2$ increasing;
- a wide band with a maximum around 3290 $cm^{-1}$ (molecular $H_2O$), contrary to $OH^-$-groups its intensity decreases with $fO_2$ increasing;
- 2 narrow bands at 3183 and 3289 $cm^{-1}$, their concentration grows with $fO_2$ decreasing;
- 2 bands at 3320 and 3398 $cm^{-1}$, their concentration grows with $fO_2$ decreasing.

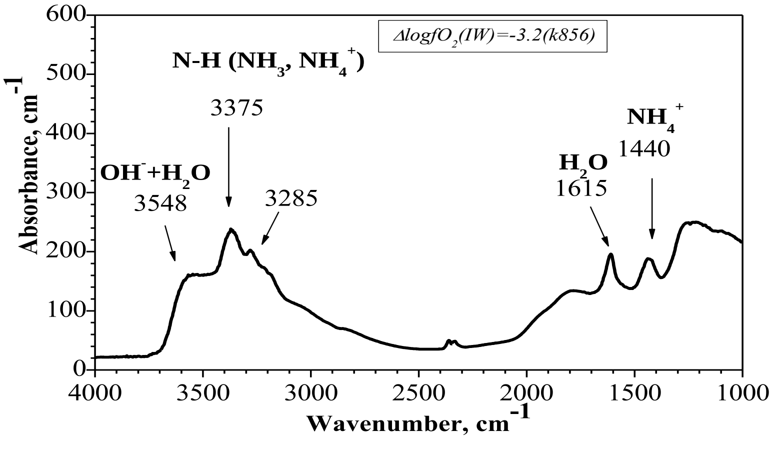

**Fig. 1:** IR spectra of N–H-bearing glasses after experiment at 4GPa, 1550°C and $fO_2$=IW-3.2.

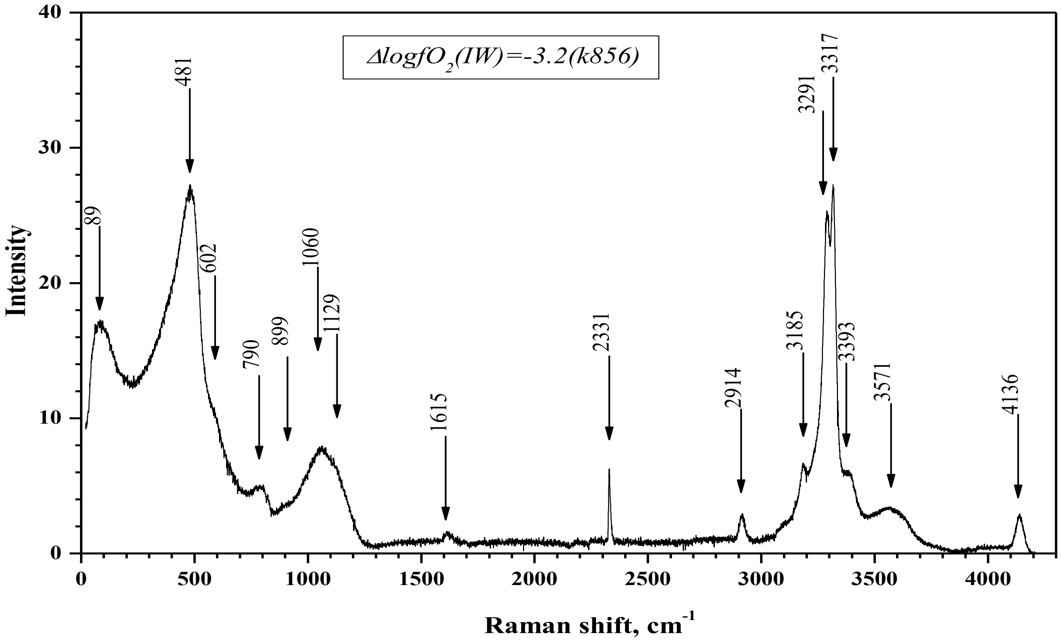

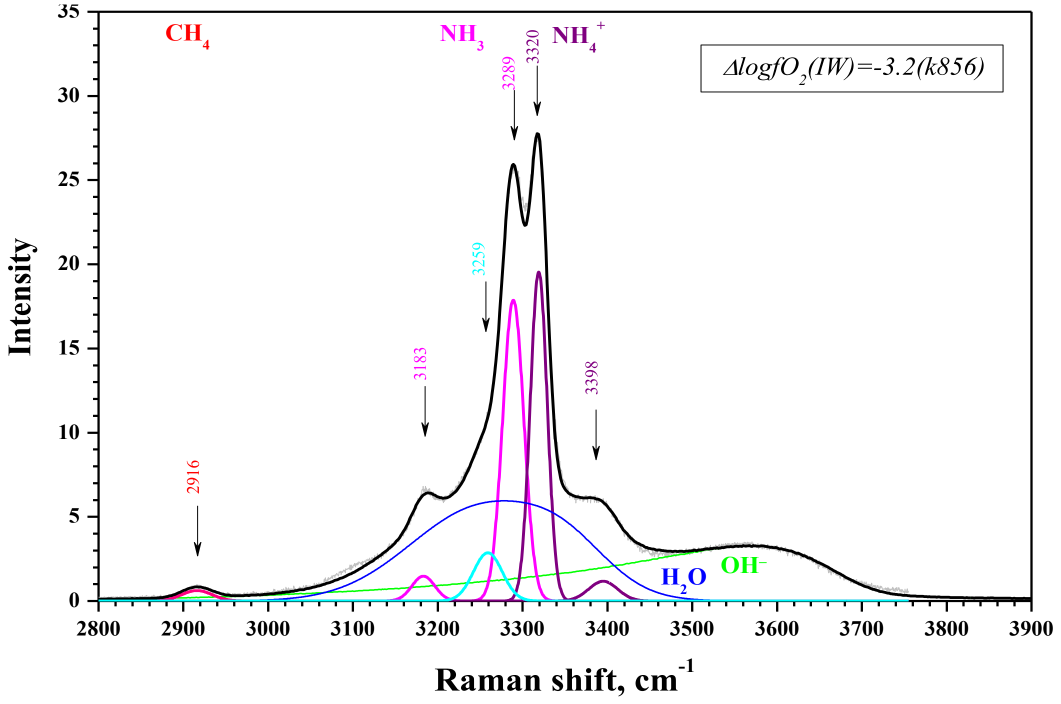

**Fig. 2:** Raman spectra of N–H-bearing glasses after experiment at 4GPa, 1550°C and $fO_2$=IW-3.2.
**Fig. 3:** Raman spectrum decomposition into composite bands (Gaussian components).

The last 4 components can be attributed to the species $NH_2^+$ (≡Si–O–$NH_2$) and $NH_2^-$ (≡Si–$NH_2$). In other interpretation these bands can characterize $NH_3$ molecule and ion $NH_4^+$ ion, respectively [Mysen et al., 2008: Mysen and Fogel, 2010].

We assume that the magmatic transport and chemical evolution of nitrogen, carbon and hydrogen during the reduced episode of early mantle evolution could be very much influenced by low $fO_2$ values in presence of the metallic Fe phase. The primary melting is a way of providing the formation of the reduced forms of nitrogen, carbon and hydrogen ($H_2$, $CH_4$, $NH_3$ together with $H_2O$, $OH^-$) in magmas of the early Earth.

The formation of N–H bonds in the reduced melts equilibrated with molten Fe alloys results in a significant increase in nitrogen solubility that should exceed 1–2 wt. %. Thus, the previous authors' assumption of probably higher nitrogen content in the reduced magma ocean in comparison with the Earth's magmas of later geological epoch [e.g., Tolstikhin et al., 1998] was verified by our experimental results.

Experimental data testify to a strong influence of pressure, $fO_2$, and hydrogen on distribution of nitrogen between metallic and silicate melts, ($D_N^{met/sil}$). It is found that at 1.5 GPa, 1400°C, log $fO_2$= IW-3.7 and 4 GPa, 1550°C, $fO_2$ = IW-3.2 the values of $D_N^{met/sil}$ are equal to 0.5 and 0.4, accordingly.

The experimental studies at a pressure corresponding to a depth of 100–150 km have shown that the self-oxidation of magma ocean with $fO_2$ increasing from IW-5 to IW-2 [Wood, B.J. et al., 2006; Javoy et al., 2010] is characterized by a decrease in the amount of species with

N–H and C-H bonds and an increase in the content of oxidized hydrogen species, such as $OH^-$ and $H_2O$. These dissolution features make $fO_2$ a critical factor in the formation of C–N–O–H volatile species during the large-scale melting of the early Earth. Our experiments allow assuming that $N_2$, $NH_3$, $CH_4$, $H_2$ and $H_2O$ could have been extracted from the reduced magma ocean and come to the surface.

*This work was made possible through support of Prog. No 28 RAS, RFBR grant No 11-05-00926a, ESD RAS project No9.*

References:

1. Kadik A.A., F.Pineau, Yu.A. Litvin, N. Jendrzejewski, I. Martinez, M. Javoy (2004). *J. Petrol.*, V.45 (7), pp.1297–1310.
2. Javoy M., E. Kaminski, F. Guyot, D. Andrault, C. Sanloup, M. Moreiraa, S. Labrosse, A Jambon, P. Agrinier, A. Davaille, C. Jaupart (2010). *Earth Planet. Sci. Lett.*, V293, pp 259–268.
3. Newman, S., E.M. Stolper & S. Epstein (1986). Measurement of water in rhyolitic glasses: Calibration of an infrared spectroscopic technique. *American Mineralogist*, 71, 1527-1541.
4. Dianov E.M., V.V. Koltashev, S.N. Klyamkin, A.R. Malosiev, O.I. Medvedkov, V.G. Plotnichenko, A.A. Rybaltovskii, A.O. Rybaltovskii, V.O. Sokolov & S.A. Vasiliev (2005). Hydrogen diffusion and *ortho-para* conversion in absorption and Raman spectra of germanosilicate optical fibers hydrogen-loaded at 150-170MPa. *Journal of Non-Crystalline Solids*, №49-51 (351**)**, 3677–3684.
5. Stolper E. (1982). Water in silicate glasses: An infrared spectroscopic study. *Contributions to Mineral Petrology*, v.81, pp. 1-17.
6. Mysen B.O., S. Yamashita, N. Cherikova (2008). Solubility and solution mechanisms of NOH volatiles in silicate melts at high pressure and temperature – amine groups and hydrogen fugacity. *Am. Mineral.*, 93, 1760–1770.
7. Mysen, B.O., M.L.Fogel (2010). Nitrogen and hydrogen isotope compositions and solubility in silicate melts in equilibrium with reduced (N+H)-bearing fluids at high pressure and temperature: Effects of melt structure. *Am. Mineral.*, 95, 987–999.
8. Mercier M. et al.(2010). Spectroscopic analysis (FTIR, Raman) of water in mafic and intermediate glasses and glass inclusions. *Geochimica et Cosmochimica Acta*, v.74, pp. 5641-5656.
9. Tolstikhin I.N., B. Marty (1998). *Chem. Geol.*, V.147, pp. 27–52.
10. Wood B.J., M.J. Walter, J.Wade (2006). *Nature*, V. 441**,** pp. 825-833.

## Lukanin O.A., Ryzhenko B.N., Kurovskaya N.A. Zinc and lead in the water-chloride magmatic fluids (to the problem of distributions of these metals between fluid phase and granite melt)

Vernadsky Institute of Geochemistry and Analytical Chemistry of RAS, Moscow

**Abstract.** The results of thermodynamic modeling in systems ZnO(PbO)-Na(K)Cl-HCl-H2O within temperature range of 600-900oC and pressures of 0.7-5 kbar show the dominance of chloride complexes of zinc and lead in water-chloride fluids at T-P-CCl-pH parameters corresponding to the conditions of magmatic fluids. They are in good agreement with available experimental data on distribution coefficients of Zn and Pb between water-chloride fluids and granitic melts (D(Zn)f/m and D(Pb)f/m), obtained at 800°C and pressures of 1-5 kb, that demonstrates: 1) D(Zn)f/m and D(Pb)f/m increase with increase of Na and K chlorides concentration in aqueous fluid; 2) a sharp increase in D(Zn)f/m and D(Pb)f/m at adding HCl to fluid phase; 3) the higher D(Zn)f/m versus D(Pb)f/m values at given T-P-X conditions. It is assumed that experimentally established effect of D(Zn)f/m and D(Pb)f/m decrease at pressure increase is caused by the increase of alkalinity of chloride aqueous fluid in equilibrium with granite melt.

*Key words: zinc, lead, magmatic fluid, chloride complexes, distribution coefficients, granite melt, thermodynamic modeling.*

**Citation:** Lukanin O.A., B.N. Ryzhenko, N.A. Kurovskaya (2013). Zinc and lead in the water-chloride magmatic fluids (to the problem of distributions of these metals between fluid phase and granite melt).

Thermodynamic modeling of equilibrium relations of complexes of zinc and lead in water-chloride fluids in systems ZnOk(PbOk)-Na(K)Cl-HCl-$H_2O$ at temperatures of 600 - 900°C and pressures of 0.7 - 5 kbar that were made earlier [Lukanin and others 2010 , 2011, 2013; Lukanin et al., 2011], provided an opportunity to assess the solubility and possible species of zinc and lead in chloride-containing aqueous fluids in *PT*- parameters of magmatic fluids of granitoid magmas. A comparison of calculated data with experimental data on Zn and Pb distribution between water-chloride fluid and granite melt largely explains the influence of various physicochemical parameters (chlorine concentration in fluid ($C_{Cl}$), pH of solution and pressure) on the distribution coefficients of Zn and Pb fluid/melt ($D(Me)^{f/m}$).

Experimental studies of Zn and Pb distribution between granite melts and water-chloride fluids performed at temperatures of 800-850$^oC$ and pressures of 1.2 - 4.5 kb show significant influence of chloride concentration, pH, and pressure on the distribution coefficients of these metals between fluid and the melt [Holland, 1972; Malinin, Khitarov, 1984; Urabe, 1985, 1987; Malinin, Kravchuk, 1991; Chevychelov et al., 1994, and others]. Despite the considerable spread of experimental data, the results of these studies revealed the following general regularities: 1) D(Zn)f/m and D(Pb)f/m increase with increase of chlorides (NaCl+KCl) concentration in aqueous fluid; 2) especially sharp increase of $D(Zn)^{f/m}$ and $D(Pb)^{f/m}$ with the addition of HCl to aqueous chloride fluid phase at *T*, *P* and $C_{Cl}$ = const; 3) the higher values of $D(Zn)^{f/m}$ compared to that of D(Pb)f/m at given *T-P-X* conditions; 4) $D(Zn)^{f/m}$ and $D(Pb)^{f/m}$ decrease with increasing of pressure at *T* and $C_{Cl}$ = const. Consider these experimentally identified patterns in the light of our results of thermodynamic modeling of relatively simple systems.

Experimentally established increase of Zn and Pb concentration in fluid and thus the degree of extraction of these elements from melt with increasing concentrations of chloride provides a basis to assume that principal species of these metals in fluid are chlorine-containing complexes. This is confirmed by the calculated data for ZnO-NaCl-HCl-$H_2O$ and PbO-NaCl-HCl-$H_2O$ systems indicating firstly that the predominant content of Zn and Pb in aqueous chloride solution exists as chloride complexes throughout the range of T-P-X-parameters under which the most number of experiments were conducted, and, secondly, about the significant ZnO and PbO solubility increase with the increase of $C_{Cl}$ and decrease of pH. The solubility of Zn and Pb oxides in these systems corresponds to the content of these metals in aqueous chloride fluid phase in equilibrium with their solid oxides at given *T*, *P* and $C_{Cl}$. If not lead and zinc oxides but other condensed phases containing ZnO and PbO as impurities (oxides, silicates, oxide melts) are in equilibrium with solution under the same conditions, the solubility of Pb and Zn in fluid obviously seems to be different. It decreases with decreasing of ZnO and PbO activity in condensed phases in case of other components of condensed phase dissolved in fluid influence is negligible and Zn and Pb chloride complexes are the predominant species in fluid phase. At the same time in *condensed phase* (containing ZnO and PbO) - *fluid* ($H_2O$-Na(K)Cl-HCl) *system* under given ZnO and PbO content the increase of chlorides concentration (*P* and *T* = const) will cause the increase of Zn and Pb solubility in fluid. For *granite melt - aqueous chloride fluid system* that means that the increase of chloride concentration and pH decrease should lead to metals concentration increase in fluid and consequently to increase of these elements fluid/melt distribution coefficients. Thus, the results of calculations of chlorine concentration and pH influence on zinc and lead contents in solutions of ZnO(PbO)-NaCl-HCl-$H_2O$ systems generally at a qualitative level are consistent with experimental data on $D(Zn)^{f/m}$ and $D(Pb)^{f/m}$ increase with chloride concentration (NaCl, KCl) increase in fluid and with HCl addition to it.

The analysis of calculated data for ZnO(PbO)-NaCl-HCl-$H_2O$ systems shows that Zn concentration is higher than that of Pb within wide range of chloride concentrations under slightly alkaline, neutral or acidic conditions (Fig. 1). This correlates well with experimental results, according to that the $D(Zn)^{f/m}$ is more than $D(Pb)^{f/m}$ at given T-P-$C_{Cl}$ conditions.

According to model calculations pressure increase promotes chloride complexes dominance and Zn and Pb concentrations increase in aqueous chloride solutions. At first glance, that contradicts the experimental data on $D(Zn)^{f/m}$ and $D(Pb)^{f/m}$ decrease with pressure increase under isothermal conditions at $C_{Cl}$ = const. However, this contradiction seems to be eliminated by taking into account the possible pressure influence on pH of fluid phase in equilibrium with granite melt. Granite material in *granite-NaCl-HCl-$H_2O$ system* has a buffering effect on pH of fluid phase as evidenced by preliminary results of thermodynamic modeling.

Thus, the results of thermodynamic modeling of ZnO(PbO)-NaCl-HCl-$H_2O$ systems, apparently do not contradict experimental data on pressure influence on $D(Zn)^{f/m}$ and $D(Pb)^{f/m}$, assuming that the tendency of fluid phase alkalinity increase with pressure increase observed in fluid–granite system, realizes for fluid-granitic melt equilibration in experimental studies as well.

The calculated data on pH change in chloride aqueous solution in equilibrium with granite depending on rock/water (R/W) mass ratio at temperature of $800^oC$ and pressure of 1, 2 and 5 kbars show that variation of R/W> 5-10, as well as adding of HCl to the solution has relatively small effect on aqueous chloride solution pH (within ± 0.25). Pressure has the greatest influence on pH of the solution of given composition under isothermal conditions particularly within the range of 2-3 kbar. Comparison of pH in the granite-fluid system with pH of pure water shows trend of alkalinity of water-chloride fluid increase with pressure at T = const.

The calculated data presented in Fig. 2 show that pH of aqueous chloride fluid equilibrated with granite decreases more slowly than that of pure water with increase of pressure from 1 to 5 kbar. If at 2 kbar fluid pH is close to neutral, then at 5 kbar fluid pH is more than one unit higher than that of pure water.

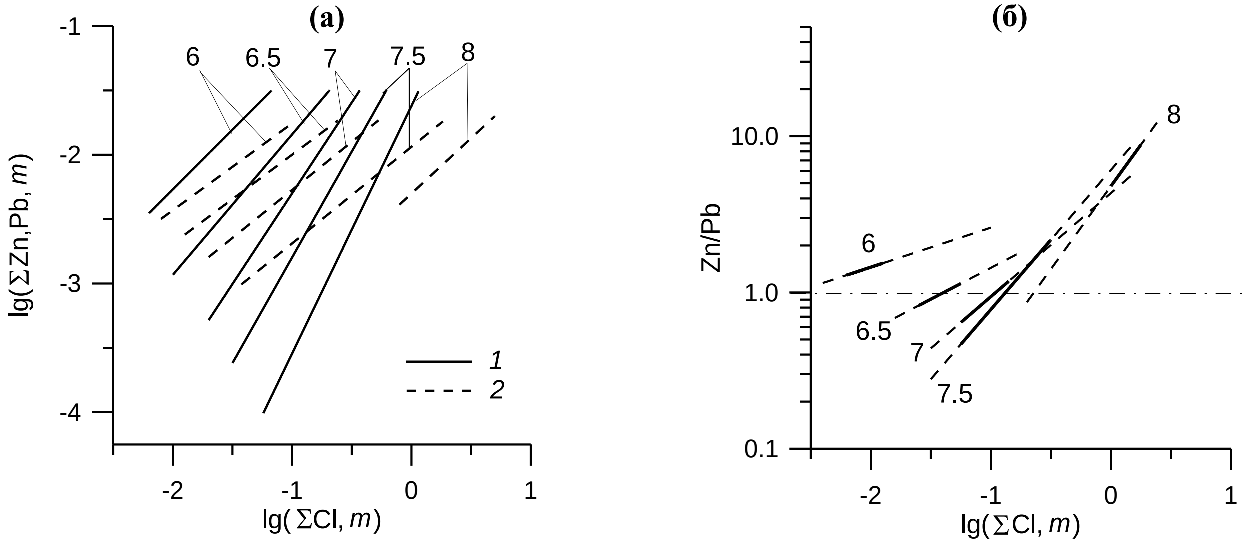

**Fig. 1.** Comparison of solubility of Pb and Zn in an aqueous chloride solution at given concentration of chlorine and pH (*T* = 800°C, *P* = 2 kbar).

*(a)* - Solubility of Zn and Pb depending on the concentration of chlorine at constant pH (*1* - total content of Zn, ZnO-NaCl-HCl-$H_2O$ system, *2* - total content of Pb, PbO-NaCl-HCl-$H_2O$ system). (*b)* - change of the molar Zn/Pb ratio in solution in equilibrium with metal oxides, depending on pH and chlorine concentration (solid thick lines on plots - data for investigated pH range and $C_{Cl}$; dashed lines - extrapolation). Numbers – pH values.

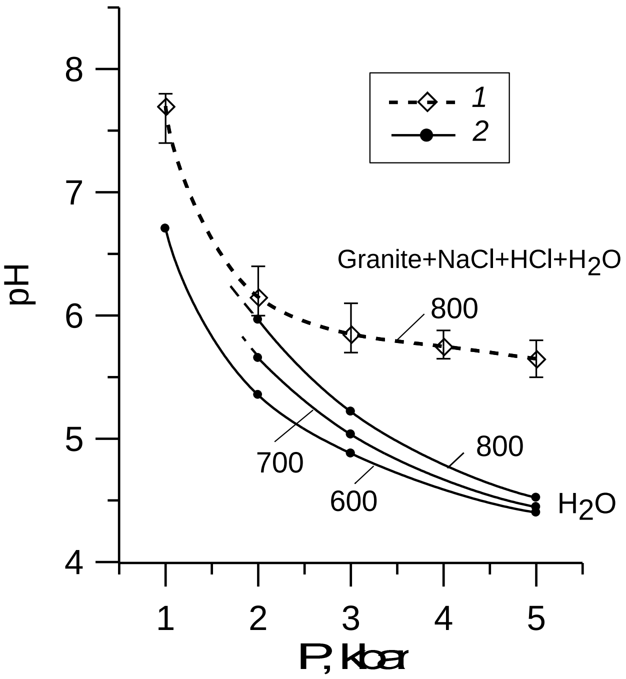

**Fig. 2.** Pressure effect on pH of "magmatic" water-chloride fluid at a temperature of 800°C.

1 – $H_2O$+NaCl+HCl fluid equilibrated with granite (averaged values for two compositions of starting solutions 1 *m* NaCl and 1 *m* NaCl + 1 *m* HCl, error interval reflects possible influence of HCl/NaCl ratio change in initial solution and R/W variations from 1 to 100);
2 - pure water pH within range of 1-5 kbar and temperatures of 600, 700 and 800°C [Borisov Shwarov, 1992].

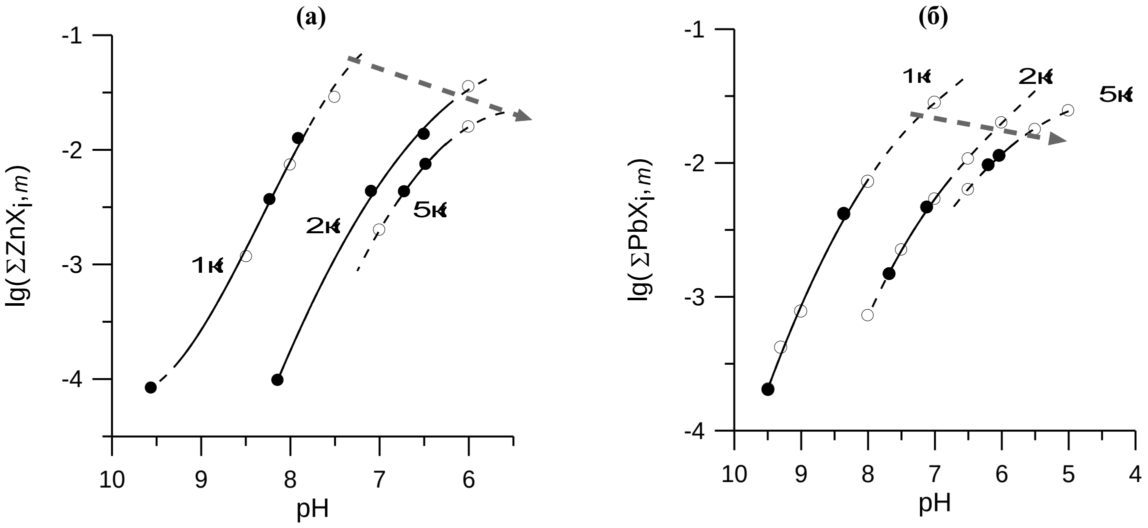

**Fig. 3.** Effect of pH on solubility of Zn (a) and Pb (b) in aqueous chloride solution with concentration of 0.1 m chlorine in ZnO(PbO)-NaCl-HCl-$H_2O$ systems at 800°C and pressures of 1, 2 and 5 kbars. Filled circles - calculated data, empty circles - data obtained from interpolation and extrapolation. Arrows schematically show the expected change in total concentrations of Zn and Pb in fluid equilibrated with granite, caused by pressure increase. Additional explanations are in the text**.**

Concurrent pressure and alkalinity increase in ZnO(PbO)-NaCl-HCl-$H_2O$ systems can be accompanied by decrease of Zn and Pb oxides solubility in fluid phase. It is the case that is schematically shown in Fig. 3 for 0.1 m NaCl solution at 800°C. Isothermal pressure increase from 1 to 5 kbar and simultaneous change of pH of approximately the same magnitude as expected according to the calculations for water-chloride fluid- granite system (from 7.3 to 5.6, Fig.2), reduces total zinc and lead concentrations in fluid.

In general, the comparison of calculated and experimental data suggests that the influence of chloride concentration, pressure and pH on Zn and Pb oxides dissolution in water-chloride solutions of relatively simple ZnO(PbO)-NaCl-HCl-$H_2O$ systems is reflected in Zn and Pb distribution coefficients between water-chloride fluid and granite melt change. However, obviously, the other factors such as variations in chemical composition of granite melt, changing the structure and melt properties with pressure and its water content increase, the presence of petrogenic elements and other magmatic volatiles besides water and chlorine in fluid phase can also provide large influence on $D(Zn)^{f/m}$ and $D(Pb)^{f/m}$ in fluid-magmatic systems.

## References:

1. Borisov M.V., Y.V. Shwarov (1992). Thermodynamics of geochemical processes. Moscow State University. 256 p. (In Russian).
2. Lukanin O.A., N.A Kurovskaya, B.N. Ryzhenko (2010). Species of Zn and Pb in water-chloride solutions at T-P conditions of fluids formation of granitoid magmas. *In: New horizons in the study of magmatic processes and ore formation. Proceedings of the conference.*, November 8-11, 2010, Moscow, IGEM, p.432-433. (In Russian).
3. Lukanin O.A., N.A. Kurovskaya, B.N. Ryzhenko (2011). The influence of Cl concentration and pH on solubility and species of Zn and Pb in water-chloride fluids at T-P parameters of granitoidic magmas degassing. *Vestnik*

*Otdelenia nauk o Zemle RAN*, Vol. 3, NZ6067, doi:10.2205/2011NZ000197.

4. Lukanin O.A., B.N. Ryzhenko, N.A Kurovskaya (2013). The solubility and species of zinc and lead in the water-chloride fluid at PT parameters corresponding to the degassing and crystallization of granitic magmas. *Geochemistry International,* No 10. (In press).
5. Malinin S.D., M.I. Khitarov (1984). Ore and major elements in the magmatic melt-fluid. *Geokhimiya,* No 2. p. 183-186. (In Russian).
6. Malinin S.D., I.F. Kravchuk (1991). The distribution of elements in equilibria involving fluids. In: Borisov A.A. et al., *Fluids and redox equilibria in magmatic systems.* M.: Nauka, Chap. 2, p. 57-117. (In Russian).
7. Chevychelov V.Y., T.P. Salov, M.B. Epelbaum (1994). Differentiation of ore elements (Pb, Zn and W, Mo) in fluid-magmatic (granitoid) system. In: *Experimental problems of geology.* M.: Nauka. 1994. p.104-121. (In Russian).
8. Lukanin O. A., N.A. Kurovskaya, B.N. Ryzhenko (2011). Solubility and species of Zn and Pb in water-chloride fluids at *TP* conditions of granite magmas degassing. *International geochemical conference Goldschmidt-2011*, August 14-19, 2011, Prague, Czech Republic. Goldschmidt Conference Abstracts. # 1366.
9. Holland H.D. (1972). Granites, solutions and base metal deposits. *Econ. Geology and Bull. of the Society of Economic Geologists,* Vol. 67, p.281-301.
10. Urabe T. (1985). Aluminous granite as source magma of hydrothermal ore deposits: an experimental study. *Econ. Geology,* Vol. 80, p.148-157.
11. Urabe T. (1987). The effect of pressure on the portioning ratios of lead and zinc between vapor and rhyolite melts. *Econ. Geology,* Vol. 82, p. 1049-1052.

## Zharkova E.V., Kadik A.A. Using oxygen electrochemical cell for the determination of equilibrium meanings of intrinsic oxygen fugacity in mineral associations

V. I. Vernadsky Institute of Geochemistry and Analytical Chemistry RAS, Moscow

**Abstract.** The values of the intrinsic oxygen fugacities obtained for the olivine, ortho and clynopiroxenes and spinels of samples of spines lherzolites are close to each other in plane of Δlog $fO_2$(sample-QFM)-$10^4$/TºK and placed between Δlog $fO_2$(WM-QFM),) and Δlog $fO_2$(IW-QFM). The values of the intrinsic oxygen fugacity testify to equilibrium character of phases of spinel lherzolites in the relationship of the chemical potential of the oxygen. The dependence of Δlog $fO_2$(sample-QFM)-$10^4$/TºK for the crystals of olivines, pyroxenes and spinels reflect the specific character of chemical state of each of them, concentration of the elements with variable valency and defects in their structure. At the same time, at the temperatures which correspond to equilibrium coexistence of the crystals must be keep the equality of the chemical potential of the oxygen in them. This is the necessary condition and may be used as geothermometer

*Key words: the intrinsic oxygen fugacity of the crystals, olivine, pyroxene, spinel, kyanite, zirkone, diamond.*

**Citation:** Zharkova E.V., A.A. Kadik (2013). Using oxygen electrochemical cell for the determination of equilibrium meanings of intrinsic oxygen fugacity in mineral associations

The estimation of the values of the intrinsic oxygen fugacity ($fO_2$) which is peculiar to redox reactions may be solved with the help of thermodynamic analysis of mineral equations, or with help of experimental determination of intrinsic oxygen fugacity of minerals of deep origin on high temperature furnace based on two solid electrolytes. Both of this methods collides with difficulties, from one hand, it's not enough hermodynamical data of the properties of mineral phases at high pressures, indeterminate modes of solid solutions, from the other hand – the degree of safety of minerals equilibrium while the xenoliths of upper mantle carry out to the surface of the Earth.

The value of the intrinsic oxygen fugacity in the crystals, glasses and basalts controlled the redox reactions in the rocks of upper mantle and in the products of their partial melting, and permit to clear up the mechanism of the differentiation of the substance while it carry out to the surface of the Earth.

The interesting using for the method of the direct determination of the intrinsic oxygen fugacity for the minerals suggested M.Sato [Sato M., 1972]. We apply this method for the investigation f different mineral associations. For example, the experiment data of the intrinsic oxygen fugacity obtained for olivine (Ol) orthopyroxene (Opx), clynopyronene (Cpx) and spinel (Spl) are close to each other in co-ordinates of Δlog $fO_2$(sample-QFM)-$10^4$/TºK and disposed between Δlog $fO_2$(WM-QFM),) and Δlog $fO_2$(IW-QFM). The values of the intrinsic oxygen fugacity testify to equilibrium character of phases of spinel lherzolites in the relationship of the chemical potential of the oxygen.

The dependence of Δlog $fO_2$(sample-QFM)-$10^4$/TºK for the crystals of olivines, pyroxenes and spinels reflect the specific character of chemical state of each of them, concentration of the elements with variable valency and defects in their structure. At the same time, at the temperatures which correspond to equilibrium coexistence of the crystals must be keep the equality of the chemical potential of the oxygen in them. This is the necessary condition and may be used as geothermometer (fig.1-6, table 1).

Based on the necessity of equality of the intrinsic oxygen fugacity of coexisting minerals, we can show, that for investigating sample of the spinel lherzolite from volcano Shavarin-Tsaram (ShTs 3-1, Mongolia, tab. 1, fig. 1) [Kadik A.A., Zharkova E.V et al., 1988] the maximum temperature of equilibrium of mineral association correspond to 1100-1050°C, and minimum temperature correspond to 900-850°C. In the table 1 and on the figures 2-6 show the other examples equilibrium and non equilibrium mineral associations from the Baikal rift zone (BRZ), fig. 3 [Kadik A.A., Zharkova E.V et al., 1994], Southen Tien Shan, fig. 4 [Kadik A.A., Zharkova E.V et al., 1995], pipe Obnazhennay fig.5, pipe “Mir” fig. 6 [Kadik A.A., Zharkova E.V et al.,1993a; Kadik A.A., Zharkova E.V et al., 1998; Kadik A.A., Zharkova E.V et al., 1993].

---

The investigation was carried out under the support of RFFI, No 11-05-92600-a.

References:

1. Kadik A.A., Zharkova E.V., Bibikova E.V., Troneva M.A. (1998). *Geokhimiya,* No 8, p. 854-860 (in Russian).
2. Kadik A.A., Zharkova E.V., Efimova E.S., Sobolev N.V.(1993). *Dokl. Akad.Nauk,* v. 328, No 3, p. 386-389 (in Russian).
3. Kadik A.A., Zharkova E.V., Kiselev A.I. (1994).DAS, v. 337, No 3, p. 100-103 (in Russian).

4. Kadik A.A., Zharkova E.V., Kovalenko V.I., Ionov D.A. (1988). *Geokhimiya*, No 6, p. 783-793 (in Russian).
5. Kadik A.A., Zharkova E.V., Lutkov V.S., Tadzhibaev G.T. *Geokhimiya*, 1995, No 8, p. 1094-1099 (in Russian).
6. Kadik A.A., Zharkova E.V., Spetsius Z.V. *DAS*, 1993, v.320, p. 217-221 (in Russian).
7. Sato M. Intrinsic oxygen fugacity of iron bearing oxide and silicate minerals under low pressure. Geol. Soc. Am. Mem. 1972. V. 135. P. 289-307.

**Table 1.** The parameters of some possible geothermometers.

| Sample | A | B | *r | **n | T equilibrium, ºC |
|---|---|---|---|---|---|
| Spinel lherzolite(ShTs 3-1), Shavarin-Tsaram, Mongolia | | | | | |
| Ol | 10.804 | 30887 | 0.991 | 10 | Ol/Opx 909.7<br>Ol/Cpx 1100.3<br>Ol/Spl 944.5 |
| Opx | 13.421 | 33982 | 0.996 | 11 | Opx/Spl 848.7 |
| Cpx | 12.481 | 33190 | 0.992 | 11 | |
| Spl | 12.468 | 32913 | 0.998 | 10 | |
| Garnet pyroxenite(ШЦ 4334-14), Shavarin-Tsaram, Mongolia | | | | | |
| Ol | 11.654 | 33464 | 0.986 | 6 | |
| Opx | 9.382 | 29872 | 0.988 | 10 | |
| Cpx | 11.28 | 32060 | 0.984 | 8 | Cpx/Opx 879.8 |
| Spl | 12.918 | 33167 | 0.999 | 11 | |
| Garnet lherzolite (313-83), Vitimskoe basalt plateau, BRZ | | | | | |
| Ol | 23.471 | 45752 | 0.994 | 9 | Ol/Opx 895.1 |
| Opx | 19.177 | 40736 | 0.996 | 9 | Ol/Cpx 941.2 |
| Cpx | 18.887 | 40186 | 0.996 | 9 | |
| "Geen"cromespinel pyroxenite (8057), South-Gissarskaiy zone, Southen Tien-Shan, pipe Tuvish | | | | | |
| Cpx | 16.256 | 38074 | 0.995 | 8 | Cpx/Spl 855.2 |
| Spl | 18.011 | 40054 | 0.996 | 9 | |
| Lherzolite with plagioclase and amphibole, pipe "Obnazhennay" (Ob 146) | | | | | |
| Ol | 9.409 | 30107 | 0.979 | 8 | Ol/CrSpl 971 |
| CrSpl | 16.211 | 38569 | 0.991 | 7 | |
| Pipe "Mir" eclogite paragenesis | | | | | |
| Ky A 909 | 17.615 | 41185 | 0.976 | 6 | |
| Zr No 19 | 13.729 | 35768 | 0.990 | 6 | |
| D AB-33 | 13.116 | 32300 | 0.989 | 9 | |

*r – coefficient of correlation; **n – number of experimental points.

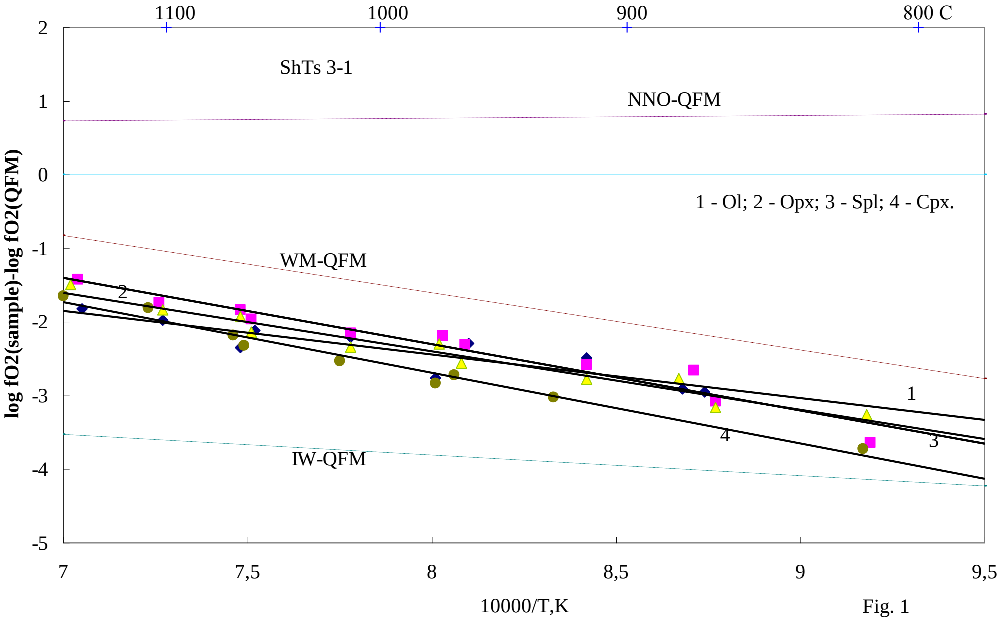

Fig. 1

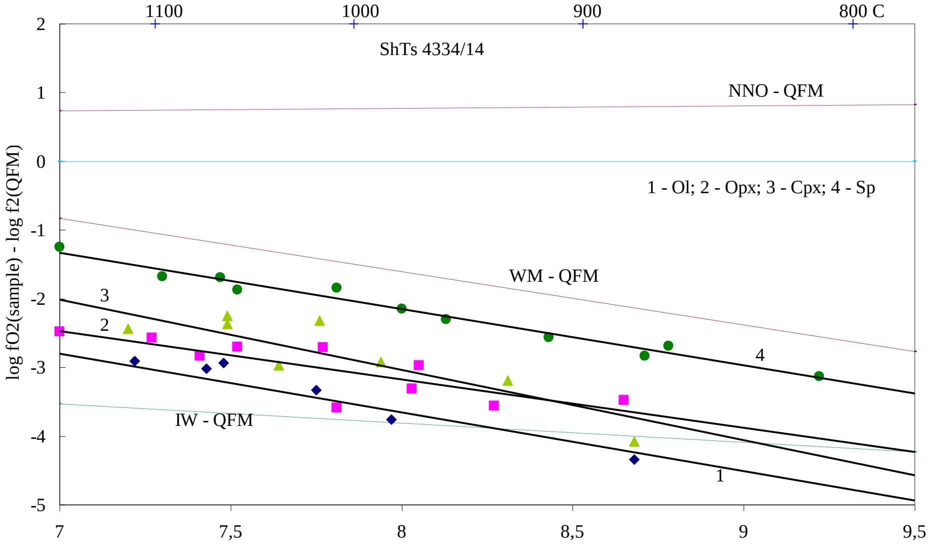

Fig .2

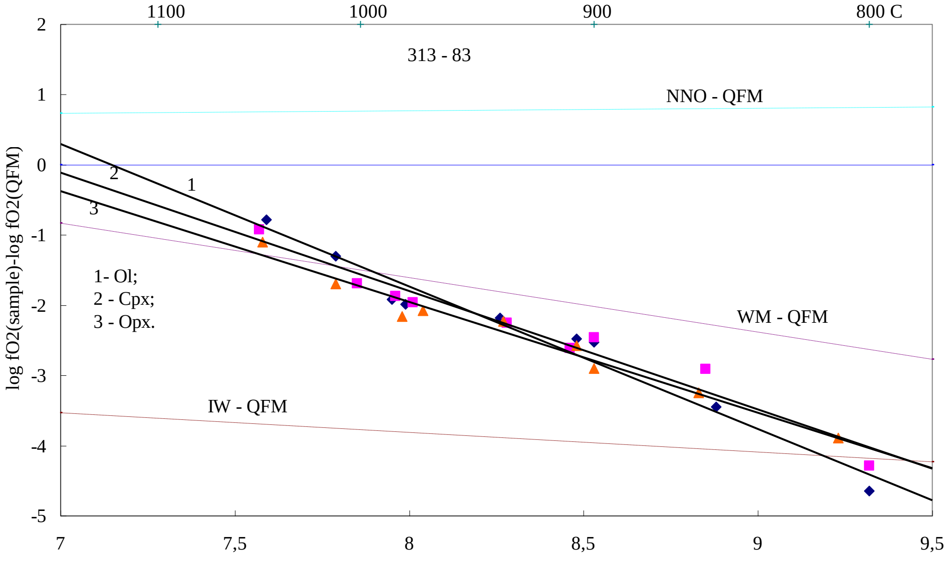

Fig. 3

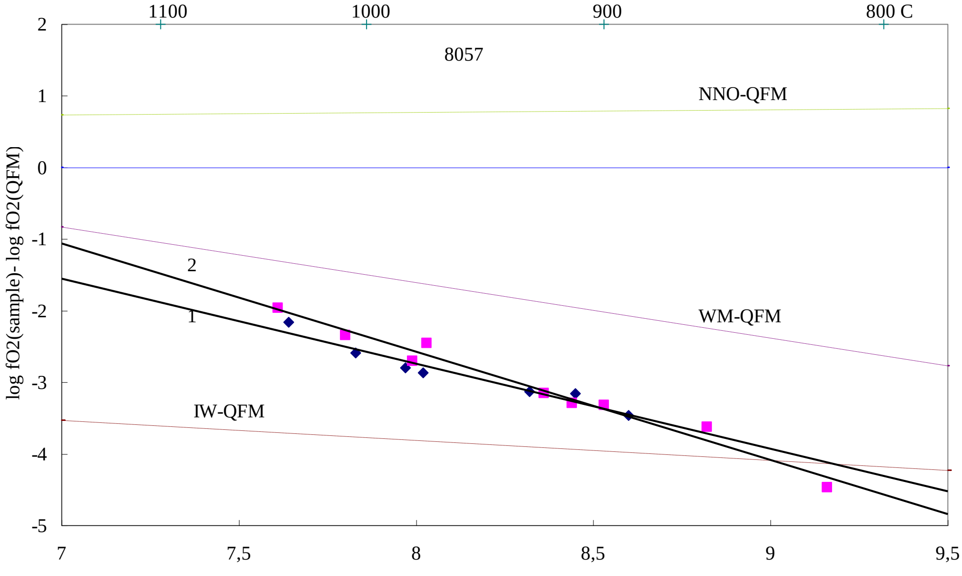

Fig. 4

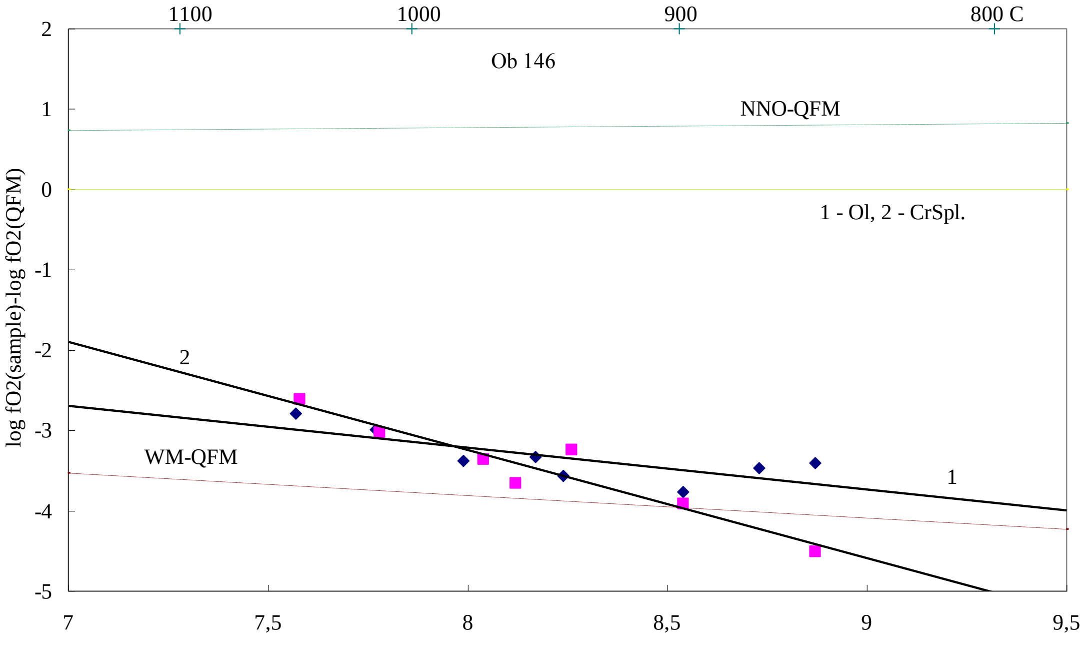
1100
1000
900
800 C
Ob 146
NNO-QFM
1 - Ol, 2 - CrSpl.
2
1
WM-QFM
log fO2(sample)-log fO2(QFM)
2
1
0
-1
-2
-3
-4
-5
7
7,5
8
8,5
9
9,5
10000/T,K

Fig. 5

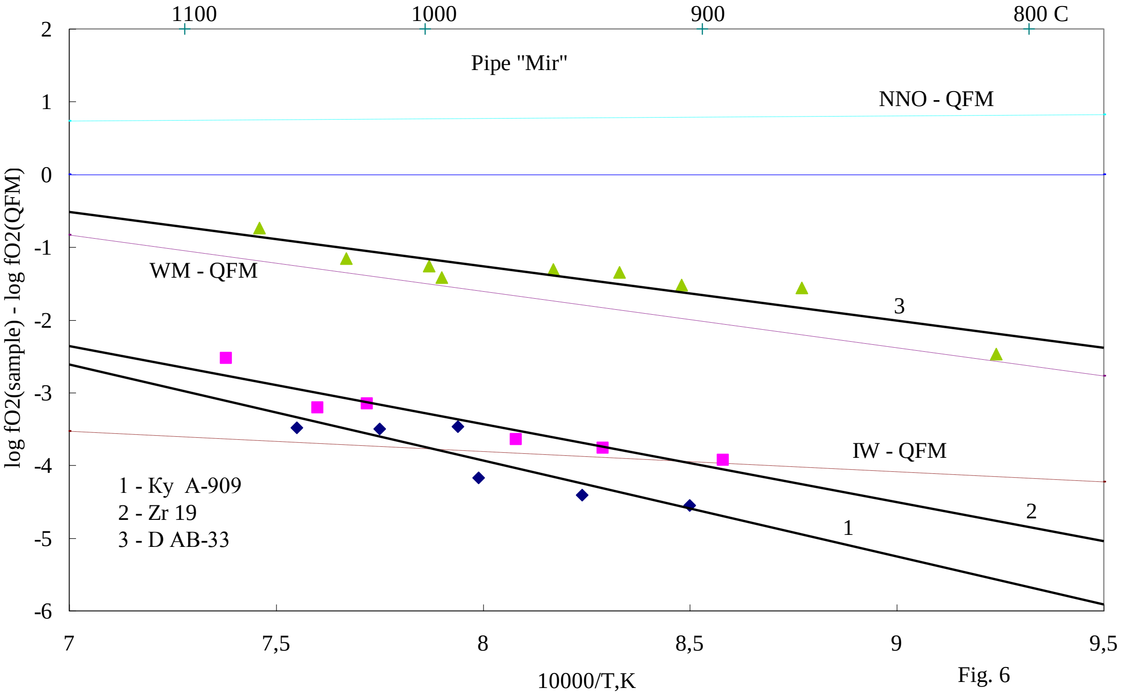
1100
1000
900
800 C
Pipe "Mir"
NNO - QFM
WM - QFM
3
IW - QFM
2
1
1 - Ky A-909
2 - Zr 19
3 - D AB-33
log fO2(sample) - log fO2(QFM)
2
1
0
-1
-2
-3
-4
-5
-6
7
7,5
8
8,5
9
9,5
10000/T,K

Fig. 6